INTERNATIONAL STANDARD

ISO 14577-1

Second edition
2015-07-15

Metallic materials — Instrumented indentation test for hardness and materials parameters —

Part 1: Test method

Matériaux métalliques — Essai de pénétration instrumenté pour la détermination de la dureté et de paramètres des matériaux —

Partie 1: Méthode d'essai

Reference number
ISO 14577-1:2015(E)

ISO copyright office
Ch. de Blandonnet 8 • CP 401
CH-1214 Vernier, Geneva, Switzerland
Tel. +41 22 749 01 11
Fax +41 22 749 09 47
copyright@iso.org
www.iso.org

Contents

Page

Foreword ..... **iv**
Introduction ..... **v**
1 Scope **1**
2 Normative references **1**
3 Symbols and designations **2**
4 Principle **4**
5 Testing machine **4**
6 Test piece **5**
7 Procedure **5**
8 Uncertainty of the results **8**
9 Test report **9**
Annex A (normative) **Materials parameters determined from the force/indentation depth data set** **11**
Annex B (informative) **Types of control use for the indentation process** **24**
Annex C (normative) **Machine compliance and indenter area function** **25**
Annex D (informative) **Notes on diamond indenters** **27**
Annex E (normative) **Influence of the test piece surface roughness on the accuracy of the results** **28**
Annex F (informative) **Correlation of indentation hardness H_{IT} to Vickers hardness** **29**
Annex G (normative) **Drift and creep rate determination** **31**
Annex H (informative) **Estimation of uncertainty of the calculated values of hardness and materials parameters** **33**
Annex I (normative) **Calculation of radial displacement correction** **43**
Bibliography **45**

Foreword

ISO (the International Organization for Standardization) is a worldwide federation of national standards bodies (ISO member bodies). The work of preparing International Standards is normally carried out through ISO technical committees. Each member body interested in a subject for which a technical committee has been established has the right to be represented on that committee. International organizations, governmental and non-governmental, in liaison with ISO, also take part in the work. ISO collaborates closely with the International Electrotechnical Commission (IEC) on all matters of electrotechnical standardization.

The procedures used to develop this document and those intended for its further maintenance are described in the ISO/IEC Directives, Part 1. In particular the different approval criteria needed for the different types of ISO documents should be noted. This document was drafted in accordance with the editorial rules of the ISO/IEC Directives, Part 2 (see www.iso.org/directives).

Attention is drawn to the possibility that some of the elements of this document may be the subject of patent rights. ISO shall not be held responsible for identifying any or all such patent rights. Details of any patent rights identified during the development of the document will be in the Introduction and/or on the ISO list of patent declarations received (see www.iso.org/patents).

Any trade name used in this document is information given for the convenience of users and does not constitute an endorsement.

For an explanation on the meaning of ISO specific terms and expressions related to conformity assessment, as well as information about ISO's adherence to the WTO principles in the Technical Barriers to Trade (TBT) see the following URL: Foreword – Supplementary information

The committee responsible for this document is ISO/TC 164, *Mechanical testing of metals*, Subcommittee SC 3, *Hardness testing*.

This second edition cancels and replaces the first edition (ISO 14577-1:2002), which has been technically revised.

ISO 14577 consists of the following parts, under the general title *Metallic materials — Instrumented indentation test for hardness and materials parameters*:

— *Part 1: Test method*

— *Part 2: Verification and calibration of testing machines*

— *Part 3: Calibration of reference blocks*

— *Part 4: Test method for metallic and non-metallic coatings*

Introduction

Hardness has typically been defined as the resistance of a material to permanent penetration by another harder material. The results obtained when performing Rockwell, Vickers, and Brinell tests are determined after the test force has been removed. Therefore, the effect of elastic deformation under the indenter has been ignored.

ISO 14577 (all parts) has been prepared to enable the user to evaluate the indentation of materials by considering both the force and displacement during plastic and elastic deformation. By monitoring the complete cycle of increasing and removal of the test force, hardness values equivalent to traditional hardness values can be determined. More significantly, additional properties of the material, such as its indentation modulus and elasto-plastic hardness, can also be determined. All these values can be calculated without the need to measure the indent optically. Furthermore, by a variety of techniques, the instrumented indentation test allows to record hardness and modulus depth profiles within a, probably complex, indentation cycle.

ISO 14577 (all parts) has been written to allow a wide variety of post-test data analysis.

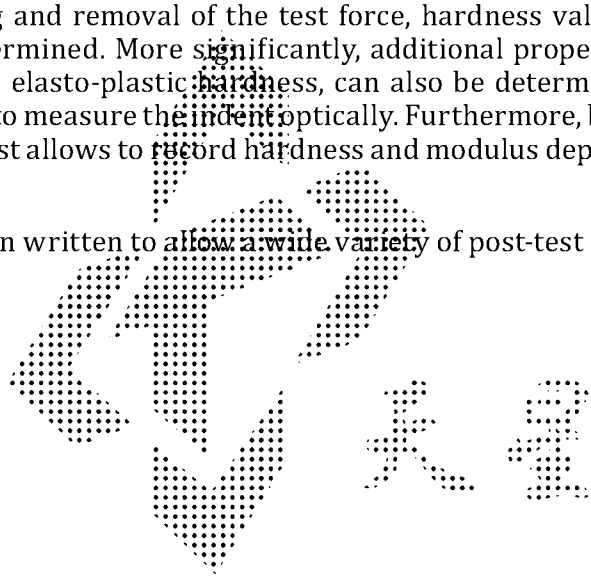

Metallic materials — Instrumented indentation test for hardness and materials parameters —

Part 1: Test method

1 Scope

This part of ISO 14577 specifies the method of instrumented indentation test for determination of hardness and other materials parameters for the following three ranges:

— macro range: 2 $N \leq F \leq 30$ kN;

— micro range: 2 $N > F$; $h > 0{,}2$ µm;

— nano range: $h \leq 0{,}2$ µm.

For the nano range, the mechanical deformation strongly depends on the real shape of indenter tip and the calculated material parameters are significantly influenced by the contact area function of the indenter used in the testing machine. Therefore, careful calibration of both instrument and indenter shape is required in order to achieve an acceptable reproducibility of the materials parameters determined with different machines.

The macro and micro ranges are distinguished by the test forces in relation to the indentation depth.

Attention is drawn to the fact that the micro range has an upper limit given by the test force (2 N) and a lower limit given by the indentation depth of 0,2 µm.

The determination of hardness and other material parameters is given in Annex A.

At high contact pressures, damage to the indenter is possible. For this reason in the macro range, hardmetal indenters are often used. For test pieces with very high hardness and modulus of elasticity, permanent indenter deformation can occur and can be detected using suitable reference materials. It is necessary that its influence on the test result be taken into account.

This test method can also be applied to thin metallic and non-metallic coatings and non-metallic materials. In this case, it is recommended that the specifications in the relevant standards be taken into account (see also 6.3 and ISO 14577-4).

2 Normative references

The following documents, in whole or in part, are normatively referenced in this document and are indispensable for its application. For dated references, only the edition cited applies. For undated references, the latest edition of the referenced document (including any amendments) applies.

ISO 14577-2:2015, *Metallic materials — Instrumented indentation test for hardness and materials parameters — Part 2: Verification and calibration of testing machines*

ISO/IEC Guide 98-3:2008, *Uncertainty of measurement — Part 3: Guide to the expression of uncertainty in measurement (GUM:1995)*

3 Symbols and designations

For the purposes of this document, the symbols and designations in Table 1 shall be applied (see also Figure 1 and Figure 2).

Table 1 — Symbols and designations

Symbol	Designation	Unit
A_p (h_c)	Projected area of contact of the indenter at distance h_c from the tip	mm^2
A_s (h)	Surface area of the indenter at distance h from the tip	mm^2
C_{IT}	Indentation creep	%
C_T	Total measured compliance of the contact (dh/dF tangent to the force removal curve at maximum test force)	nm/mN
C_F	Instrument compliance	nm/mN
C_S	Compliance of the contact after correction for machine compliance	nm/mN
E_{IT}	Indentation modulus of the test piece	GPa
E_r	Reduced plane strain modulus of the contact (combination of test piece and indenter plane strain moduli)	GPa
F	Test force	N
F_{max}	Maximum test force	N
h	Indentation depth under applied test force	mm
h_c	Depth of the contact of the indenter with the test piece at F_{max}	mm
h_{max}	Maximum indentation depth at F_{max}	mm
h_p	Permanent indentation depth after removal of the test force	mm
h_r	Point of intersection of the tangent c to curve b at F_{max} with the indentation depth-axis as identified on Figure 1	mm
H_{IT}	Indentation hardness	GPa
HM	Martens hardness	GPa
HM_S	Martens hardness, determined from the slope of the increasing force/indentation depth curve	GPa
HM_{diff}	Martens hardness, determined from the first derivative of h vs $\sqrt{F}$	GPa
ν_S	Poisson's ratio of the test piece	
r	Radius of spherical indenter	mm
R_{IT}	Indentation relaxation	%
W_{elast}	Elastic reverse deformation work of indentation	N·m
W_{total}	Total mechanical work of indentation	N·m
α	Cone semi-angle or angle of facet to the indentation axis for pyramidal indenters	°
θ	Maximum angle between the contact surface and the indenter for calculation of radial displacement	°
η_{IT}	Ratio W_{elast}/W_{total}	%

NOTE 1 To avoid very long numbers, the use of multiples or sub-multiples of the units is permitted.

NOTE 2 The continued use of the unit N/mm^2 is allowed. 1 MPa = 1 N/mm^2.

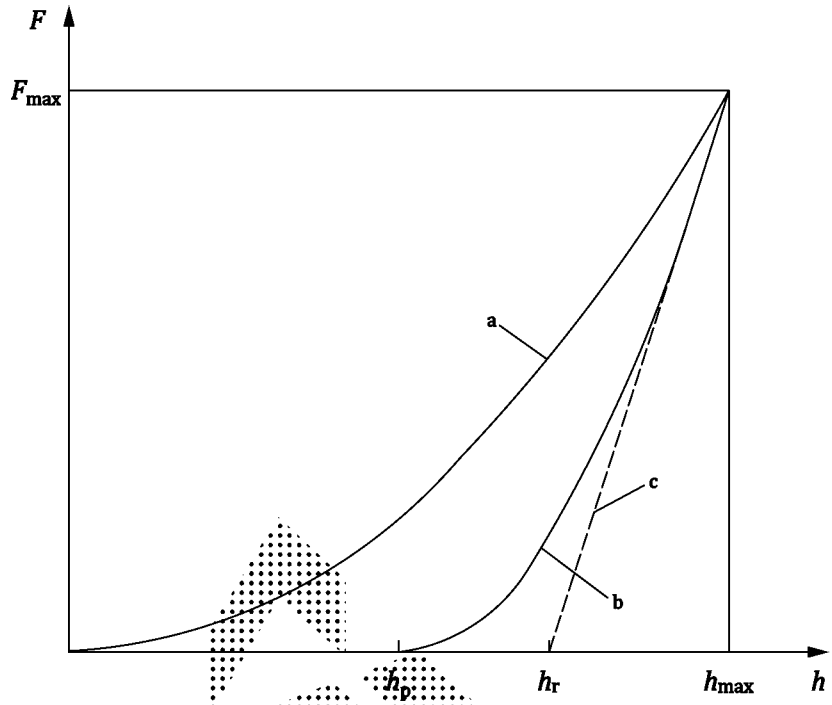

Key

a application of the test force

b removal of the test force

c tangent to curve b at F_{max}

Figure 1 — Schematic representation of the test procedure

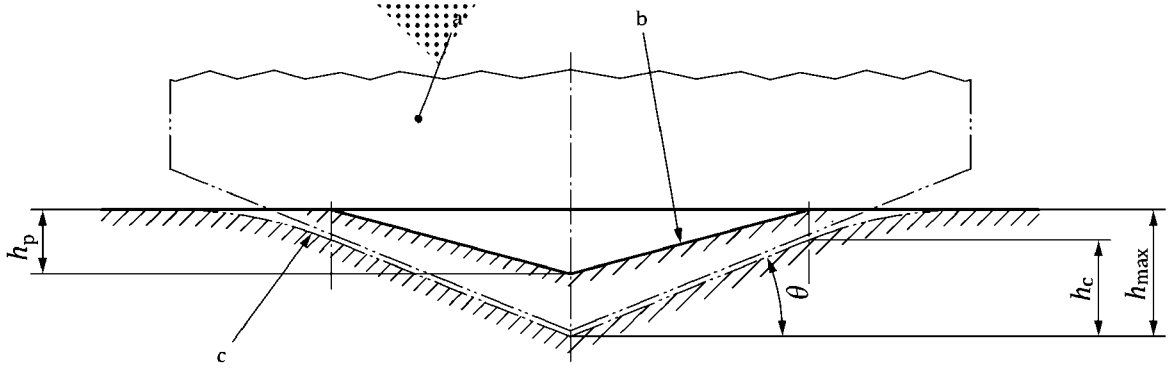

Key

a indenter

b surface of residual plastic indentation in a test piece that has a "perfectly plastic" response

c surface of test piece at maximum indentation depth and test force

θ maximum angle between the test piece surface and the indenter

Figure 2 — Schematic representation of the cross section of indentation in the case of material "sink-in"

4 Principle

Continuous recording of the force and the depth of indentation permits the determination of hardness and material properties (see Figure 1 and Figure 2). An indenter consisting of a material harder than the material under test shall be used. The following shapes and materials can be used:

a) diamond indenter shaped as an orthogonal pyramid with a square base and with an angle $\alpha = 68°$ between the axis of the diamond pyramid and one of the faces (Vickers pyramid; see Figure A.1);

b) diamond pyramid with triangular base (e.g. modified Berkovich pyramid with an angle $\alpha = 65{,}27°$ between the axis of the diamond pyramid and one of the faces; see Figure A.1);

c) hardmetal ball (especially for the determination of the elastic behaviour of materials);

d) diamond spherical tipped conical indenter.

This part of ISO 14577 does not preclude the use of other indenter geometries; however, care should be taken in interpreting the results obtained with such indenters. Other materials like sapphire can also be used.

NOTE Due to the crystal structure of diamond, indenters that are intended to be spherical are often polyhedrons and do not have an ideal spherical shape.

The test procedure can either be force-controlled or displacement-controlled. The test force, F, the corresponding indentation depth, h, and time are recorded during the whole test procedure. The result of the test is the data set of the test force and the relevant indentation depths as a function of time (see Figure 1 and Annex B).

For a reproducible determination of the force and corresponding indentation depth, the zero point for the force/indentation depth measurement shall be assigned individually for each test (see 7.3).

Where time-dependent effects are being measured

— using the force-controlled method, the test force is kept constant over a specified period and the change of the indentation depth is measured as a function of the holding time of the test force (see Figures A.3 and B.1), and

— using the indentation depth controlled method, the indentation depth is kept constant over a specified period and the change of the test force is measured as a function of the holding time of the indentation depth (see Figures A.4 and B.2).

The two kinds of control mentioned give essentially different results in the segment b of the curves in Figure B.1 a) and Figure B.2 b) or in Figure B.1 b) and Figure B.2 a).

5 Testing machine

5.1 The testing machine shall have the capability of applying predetermined test forces or displacements within the required scope and shall fulfil the requirements of ISO 14577-2.

5.2 The testing machine shall have the capability of measuring and reporting applied force, indentation displacement and time throughout the testing cycle.

5.3 The testing machine shall have the capability of compensating for the machine compliance and of utilizing the appropriate indenter area function (see Annex C and ISO 14577-2:2015, 4.5 and 4.6).

5.4 Indenters for use with testing machines can have various shapes, as specified in ISO 14577-2 (for further information on diamond indenters, see Annex D).

5.5 The testing machine shall operate at a temperature within the permissible range specified in 7.1 and shall maintain its calibration within the limits specified in ISO 14577-2:2015, Clause 4.

6 Test piece

6.1 The test shall be carried out on a region of the test surface that allows the determination of the force/indentation depth curve for the respective indentation range within the required uncertainty. The contact area shall be free of fluids or lubricants except where this is essential for the performance of the test, in which case, this shall be described in detail in the test report. Care shall be taken that extraneous matter (e.g. dust particles) is not incorporated into the contact.

Generally, provided the surface is free from obvious surface contamination, cleaning procedures should be avoided. If cleaning is required, it shall be limited to the following methods to minimize damage:

— application of a dry, oil-free, filtered gas stream;

— application of a subliming particle stream of CO_2 (but keeping the surface temperature above the dew point);

— rinsing with a solvent (which is chemically inert to the test piece) and then setting it to dry.

If these methods fail and the surface is sufficiently robust, wipe the surface with a lint-free tissue soaked in solvent to remove trapped dust particles, after which, the surface shall be rinsed in a solvent as above.

Ultrasonic methods are known to create or increase damage to surfaces and coatings and should only be used with caution.

For an explanation concerning the influence of the test piece roughness on the uncertainty of the results, see Annex E. Surface finish has a significant influence on the test results.

The test surfaces shall be normal to the test force direction. It is recommended that the test surface tilt is less than 1°. Tilt should be included in the uncertainty calculation.

6.2 Preparation of the test surface shall be carried out in such a way that any alteration of the surface hardness and/or surface residual stress (e.g. due to heat or cold working) is minimized.

Due to the small indentation depths in the micro and nano range, special precautions shall be taken during the test piece preparation. A polishing process that is suitable for the particular materials shall be used.

6.3 The test piece thickness shall be large enough (or indentation depth small enough) such that the test result is not influenced by the test piece support. The test piece thickness should be at least 10 × the indentation depth or 3 × the indentation diameter (see 7.7), whichever is greater.

When testing coatings, the coating thickness should be considered as the test piece thickness. For testing coatings, see ISO 14577-4.

NOTE The above are empirically based limits. The exact limits of influence of support on test piece depend on the geometry of the indenter used and the materials properties of the test piece and support.

7 Procedure

7.1 The temperature of the test shall be recorded. Typically, tests are carried out in the range of ambient temperatures between 10 °C and 35 °C.

The temperature stability during a test is more important than the actual test temperature. Any calibration correction applied shall be reported along with the additional calibration uncertainty. It is recommended that tests, particularly in the nano and micro ranges, be performed in controlled conditions, in the range (23 ± 5) °C and (45 ± 10) % relative humidity.

The individual tests, however, shall be carried out at stable temperature conditions because of the requirement of high depth measuring accuracy. This means that

— the test pieces shall have reached the ambient temperature before testing,

— the testing machine shall have reached a stable working temperature (operating manual should be consulted),

— the ambient, instrument, and test temperature shall be within the range for which the machine calibration is valid, and

— other external influences causing temperature changes during individual test have been controlled.

To minimize thermally induced displacement drift, the temperature of the testing machine shall be adequately maintained over the time period of one testing cycle, or a displacement drift shall be measured and corrected. A decision tree to assist in estimating the drift during the experiment is shown in Figure 3. If the drift rate is significant, the displacement data shall be corrected by measuring the drift rate during a hold at an applied force as close to zero force as is practicable or during a hold at a suitable place in the force removal curve (see ISO 14577-2:2015, Annex G and 4.3.3). If a contact in the fully elastic regime can be obtained, a hold at initial contact is preferred. In this way, material influences (creep, visco-plasticity, cracking) can be minimized. The uncertainty due to the drift, or in the drift correction used, shall be reported.

NOTE To determine the drift of surface referenced instruments, elastic contact between the reference and the surface is sufficient; contact of the indenter with the surface is not required and is not recommended.

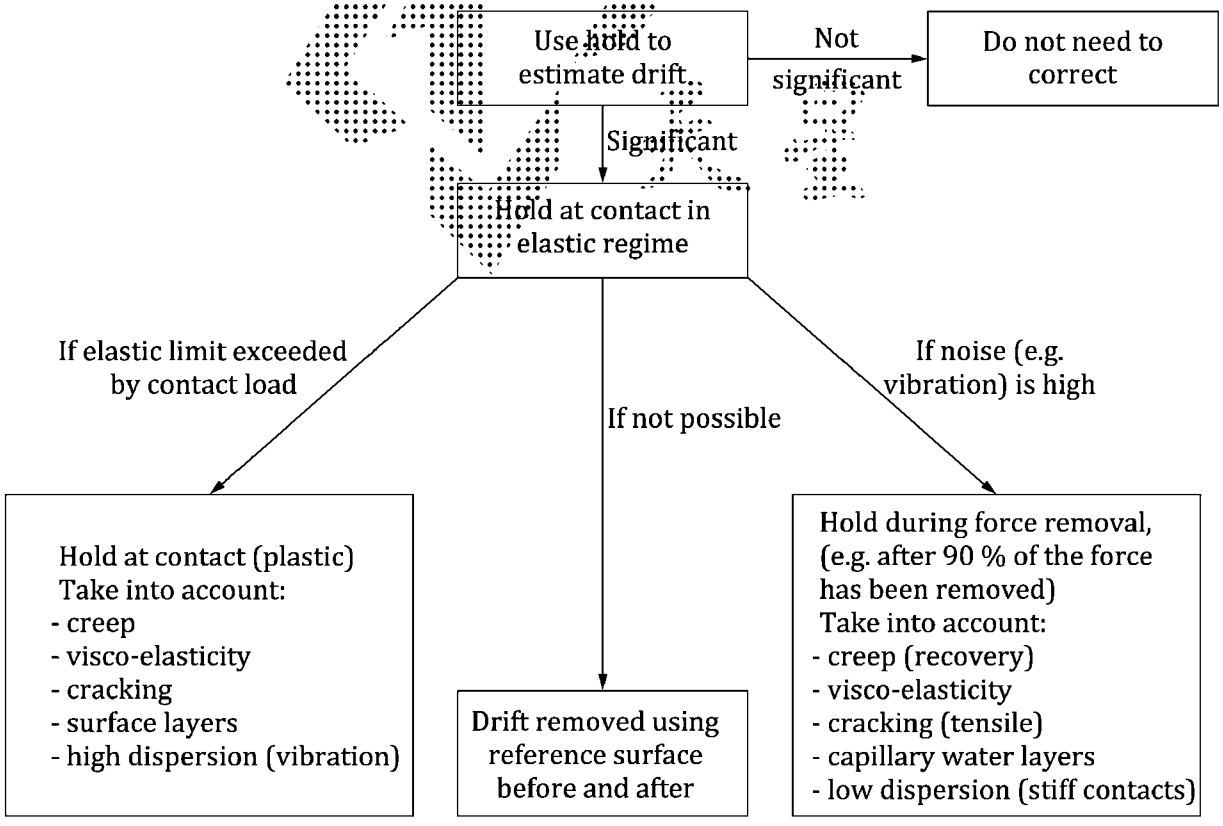

Figure 3 — Decision tree to assist in estimating thermal drift using a constant force hold period

7.2 The test piece shall be firmly supported such that there is no significant increase in the testing machine compliance. The test piece shall either be placed on a support that is rigid in the direction of indentation or be fixed in a suitable test piece holder. The contact surfaces between test piece support and test piece holder shall be free from extraneous matter, which can increase the compliance (reduce the stiffness) of the test piece support.

NOTE If the sample is supported by materials or mounting methods other than those used when determining the machine compliance, then the different elastic response of these materials and mounting methods can cause additional compliance.

7.3 The zero point for the measurement of the force/indentation depth curve shall be assigned individually to each test data set by one of the methods following. It represents the first touch of the indenter with the test piece surface. The uncertainty in the zero-point shall be reported. The uncertainty in the assigned zero point should not exceed 1 % of maximum indentation displacement for the macro and micro ranges. The zero point uncertainty for the nano range can exceed 1 %, in which case the value shall be estimated.

a) Method 1: The zero-point is calculated by extrapolation of a fitted function to the force-application curve (see curve a in Figure 1); a power law fit with the exponent as a fitting parameter constrained to be $1 \leq m \leq 2$ is recommended. The fit shall be applied to values within the range from the first recorded data point to not more than 10 % of the maximum indentation depth. The first recorded data point shall be less than 2 % of F_{max} or less than 5 % of the maximum indentation depth and the fitted data shall not contain a change in indentation response such as the onset of plastic yielding. It is recommended that the first recorded data point be as close to the zero point as possible. The uncertainty of the calculated zero point results from the fit parameters, the fitting function and the length of extrapolation. The uncertainty is calculated as the standard error of the intercept of the fit with the zero force axes.

   NOTE 1 The first part of the indentation curve (for instance up to 5 % of h_{max}) can be affected by vibration or other noise.

b) Method 2: The zero-point is the touch point determined from the first increase of either the test force or the contact stiffness. At this touch point, the step size in force or displacement shall be small enough such that the zero point uncertainty is less than the limit required.

   NOTE 2 Typical small force steps values for the macro range are 10^{-4} F_{max} and for the micro and nano range less than 5 μN.

7.4 The testing cycle can be either force-controlled or displacement-controlled. The controlled parameters can vary either continuously or step by step. A full description of all parts of the testing cycle shall be stated in the report, including the following:

a) nature of the control (i.e. force or displacement control and whether a stepped or continuous change in the controlled parameters);

b) maximum force (or displacement);

c) force application (or displacement) function;

d) length and position of each hold period;

e) data logging frequency (or number of data points).

NOTE An example cycle for nano and micro ranges is the following: force application time, 30 s; hold at F_{max}, 30 s; force removal 10 s. A 60 s hold period to measure thermal drift can also be required (see Annex G).

The time taken for a test can influence the results obtained. In order to obtain comparable test results the time taken for the test shall be taken into account.

7.5 The test force shall be applied, without shock or vibration that can significantly affect the test results, until either the applied test force or the indentation displacement attains the specified value. Force and displacement shall be recorded at the time intervals stated in the report.

During the determination of the touch point of the indenter with the test piece, the approach speed of the indenter should be low in order that the mechanical properties of the surface are not changed by the

impact. For micro range indentations, it should not exceed 2 µm/s. Typical micro/nano range approach speeds are 10 nm/s to 20 nm/s or less during final approach.

NOTE At present, the exact limit of the approach speed for the macro range is not known. It is recommended that users report the approach speed.

Force/indentation depth/time data sets are directly comparable only if the same indenter and test cycle (profile) is used. The test profile shall be specified in terms of either applied test force or indentation displacement as a function of time. The two most common cycles are

a) constant applied test force rate, and

b) constant indentation displacement rate.

The rate of applied test force removal is subject to the requirements that: a sufficient number of data points for any subsequent analysis are recorded during applied test force removal, and that the total creep and any residual creep rate is within acceptable limits (see Annex G).

If the drift rate is significant (see 7.1 and Annex G), the force and depth data shall be corrected by use of the measured drift rate.

7.6 Throughout the test, the testing machine shall be protected from shock and vibration, air movements and variations in temperature, which can significantly influence the test result.

7.7 It is important that the test results are not affected by the presence of an interface, free surface or by any plastic deformation introduced by a previous indentation in a series. The effect of any of these depends on the indenter geometry and the materials properties of the test piece. Indentations shall be at least three times their indentation diameter away from interfaces or free surfaces and the minimum distance between indentations shall be at least five times the largest indentation diameter.

The indentation diameter is the in-plane diameter at the surface of the test piece of the circular impression of an indent created by a spherical indenter. For non-circular impressions, the indentation diameter is the diameter of the smallest circle capable of enclosing the indentation. Occasional cracking can occur at the corners of the indentation. When this occurs, the indentation diameter should enclose the crack.

The minimum distances specified are best applicable to ceramic materials and metals such as iron and its alloys. For other materials, it is recommended that separations of at least 10 indentation diameters be used.

If in doubt, it is recommended that the values from the first indentation are compared with those from subsequent indentations in a series. If there is a significant difference, the indentations might be too close and the distance should be increased. A factor of two increases in separation is suggested.

It can be desirable to measure thin coatings in cross-section (e.g. to avoid problems due to surface roughness). In this case, there might not be enough coating thickness to meet the minimum spacing requirements as specified above. Smaller spacing can be used if there is experimental evidence that this does not significantly influence the force/indentation depth/time data sets with respect to correctly spaced indentations on similar test pieces with thicker coatings.

8 Uncertainty of the results

A complete evaluation of the uncertainty shall be carried out in accordance with ISO/IEC Guide 98-3. A detailed description of two methods of evaluation of uncertainty is given in Annex H.

Method 1: This approach for determining uncertainty considers only those uncertainties associated with the overall measurement performance of the testing machine with respect to reference blocks (abbreviated as CRM below). These performance uncertainties reflect the combined effect of all of the separate uncertainties (indirect verification). When using this approach, it is important that, during the test, the individual machine components are operating in the exactly same way and within the tolerances of the indirect validation being used to estimate the uncertainties.

Method 2: This approach calculates a combined uncertainty from individual contributions. These can be grouped into random and systematic uncertainties. Individual parameters can contribute one or both types of uncertainty to the total measurement uncertainty. For example, the uncertainty in measured displacement can have a random component due to the resolution of the scale used and vibrational noise, etc., plus a systematic component due to the displacement sensor calibration uncertainty. The following sources of uncertainty shall be considered:

— zero point assignation;

— measurement of force and displacement (i.e. noise floor, including effects of ambient vibrations and magnetic field strength changes etc.);

— fitting of the force-removal curve;

— thermal drift rate;

— contact area due to surface roughness;

— force, displacement;

— testing machine compliance;

— indenter area function calibration values;

— calibration drift due to uncertainty in temperature of testing machine and time since last calibration;

— tilt of test surface.

It might not always be possible to individually quantify all of the identified contributions to the random uncertainty. In this case, an estimate of standard uncertainty can be obtained from the statistical analysis of repeated indentations into the test material. Care should be taken that systematic standard uncertainties that can contribute to the random standard uncertainty are not counted twice (see ISO/IEC Guide 98-3:2008, Clause 4).

A guideline for the evaluation of the uncertainty in determination of hardness and materials parameters (Annex A) is given in Annex H.

9 Test report

The test report shall include the following information:

a) reference to this part of ISO 14577, i.e. ISO 14577-1:2015;

b) all details necessary for identifying the test piece;

c) material and shape of the indenter and, where used, the detailed area function of the indenter;

d) testing cycle (control method and full description of the cycle profile); this should include

   1) set point values,

   2) rates and times of force or displacement,

   3) position and length of hold points, and

   4) data logging frequency or number of points logged for each section of the cycle;

e) result obtained, the total expanded uncertainty and the number of tests;

f) method and functional form of any fit used for the determination of the zero-point;

g) all operations not specified by this part of ISO 14577, or regarded as optional;

h) details of any occurrence that can have affected the results;

i) temperature of the test;

j) date and time of test;

k) analysis methods;

l) if required, all agreed additional information including determined values from the measured force/indentation depth curve and detailed information about the uncertainty budget.

NOTE It is frequently desirable to describe in the test report the location of the indentation on the test piece and the unique identifier of the instrument or the specific instrument configuration used to perform the test.

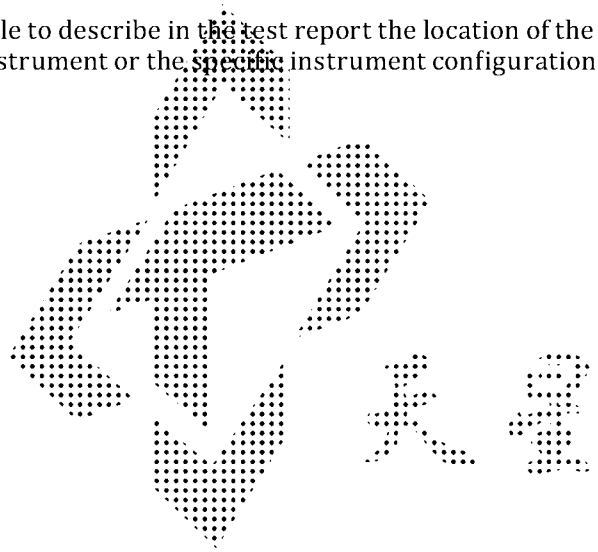

Annex A
(normative)

Materials parameters determined from the force/indentation depth data set

A.1 General

Instrumented indentation force/indentation depth data sets can be used to derive a number of materials parameters.

NOTE Using more complex test procedures, like extended cycles (load-partial unload) in an indentation that increases incrementally in force to obtain many unloading curves referenced to the same zero point, it is possible to get information about contact compliance at different test forces at a single test site.

A.2 Martens hardness[1)]

A.2.1 Determination of Martens hardness, HM

Martens hardness, HM, is measured under applied test force. Martens hardness is determined from the values given by the force/indentation depth curve during the increasing of the test force, preferably after reaching the specified test force. Martens hardness includes the plastic and elastic deformation, thus this hardness value can be calculated for all materials.

Martens hardness is defined for the Vickers and Berkovich pyramidal indenters shown in Figure A.1. It is not defined for the Knoop indenter or for ball indenters.

Martens hardness is defined as the test force, F, divided by $A_s(h)$, the surface area of the indenter penetrating beyond the zero-point of the contact, and is expressed in MPa, as given in Formula (A.1).

$$\mathrm{HM} = \frac{F}{A_s(h)} \tag{A.1}$$

NOTE The formula gives HM in MPa. To get HM in GPa a factor of 10^{-3} is required.

Values of Martens hardness are comparable only if obtained at the same depth.

The designation of angle α for the Vickers and Berkovich indenters is shown in Figure A.1.

The surface area $A_s(h)$ for the Vickers indenter is given in Formula (A.2) and for the Berkovich indenter in Formula (A.3).

a) Vickers indenter

$$A_s(h) = \frac{4 \times \sin\alpha}{\cos^2\alpha} \times h^2 \tag{A.2}$$

b) Berkovich indenter

$$A_s(h) = \frac{3 \times \sqrt{3} \times \tan\alpha}{\cos\alpha} \times h^2 \tag{A.3}$$

1) Former designation Universal hardness HU, see Reference [1].

NOTE 1 $A_S(h) = 26{,}43 \times h^2$ for the Vickers indenter ($2\alpha = 136°$), $A_S(h) = 26{,}43 \times h^2$ for the original Berkovich indenter ($\alpha = 65{,}03°$) and $A_S(h) = 26{,}98 \times h^2$ for the modified Berkovich indenter ($\alpha = 65{,}27°$).

NOTE 2 Most Berkovich indenters in use have, in fact, a modified Berkovich geometry.

For an indentation depth $h < 6$ µm, the area function of the indenter cannot be assumed to be that of the perfect theoretical shape, since all pointed indenters have some degree of rounding at the tip and spherically ended indenters (spherical and conical) are unlikely to have a uniform radius. The determination of the exact area function for a given indenter is particularly important for these indentation depths, but is beneficial for all indentation depths (see ISO 14577-2:2015, 4.5.1 and 4.6).

For an indentation depth $h < 6$ µm, the real surface area, $A_S(h)$, shall be used for the calculation; see Annex C and Reference [2].

NOTE 3 The area function, $A_S(h)$, is normally expressed as a mathematical function relating the surface area to the distance from the tip of the indenter. Where the area function cannot be described by a relatively simple (cubic or polynomial) mathematical function, then an estimate can be made either graphically or by using a look-up table. Alternatively, a different mathematical function can be used to describe different parts of the indenter or a spline function adopted.[21]

For the micro and macro ranges, the test forces, 1 N, 2,5 N, 5 N, and 10 N and their decimal multiples should be chosen for easy comparison of hardness values.

For certain applications, it can be useful to hold the specified test force over a specific time interval. The duration of the hold period of the test force should be documented to an accuracy of 0,5 s. The field of application for Martens hardness is given in Figure A.2.

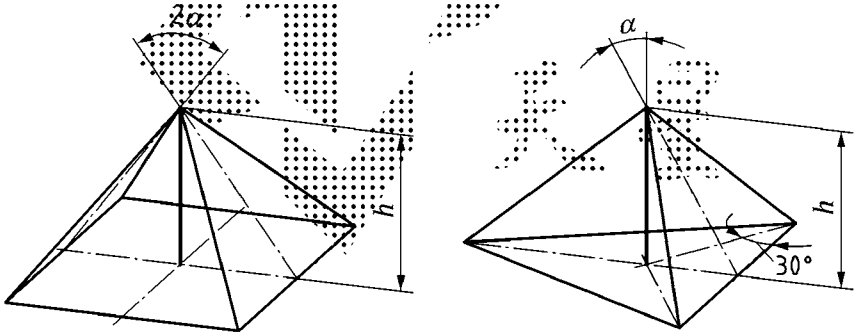

Figure A.1 — Shape of indenters for determination of HM

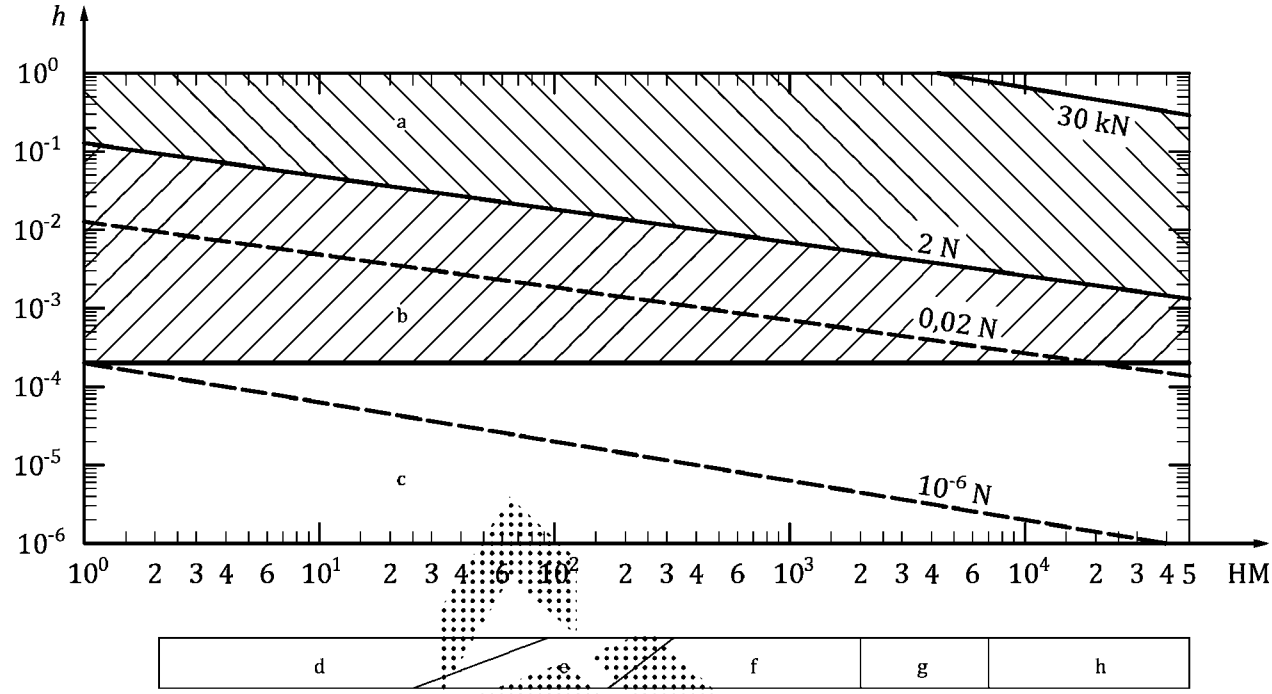

Key

a	macro range	e	plastics
b	micro range	f	non-ferrous metals
c	nano range	g	steel
d	rubber	h	hardmetals; ceramics

NOTE HM is given in megapascals in Figure A.2

Figure A.2 — Relationship between Martens hardness, indentation depth, and test force

A.2.2 Designation of Martens hardness

EXAMPLE

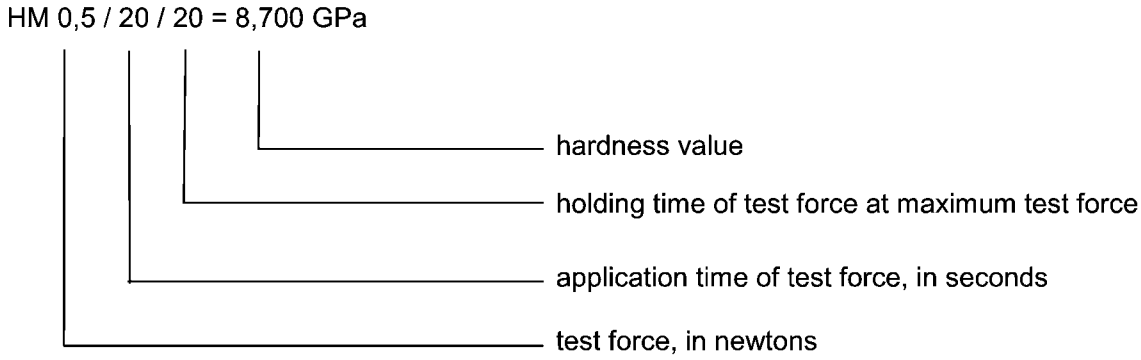

A.3 Martens hardness, determined from the increasing force/indentation depth curve

A.3.1 Determination of Martens hardness from the slope of the increasing force/indentation curve, HM_S

For homogeneous materials (where the dimension of the inhomogeneities in the region of surface is small in relation to the indentation depth), Formula (A.4) is a reasonable approximation to the force/indentation depth curve for force – displacement data between 50 % F_{max} and 90 % F_{max}:

$$h = m_s \times \sqrt{F} \tag{A.4}$$

The slope, m_s can be determined by a linear regression of the Formula (A.4) in the range 50 % $F_{max} < F <$ 90 % F_{max}. In this case, it is possible to determine the hardness by the modified method given in Formula (A.5) from the force/indentation depth curve:

$$HM_S = \frac{1}{{m_s}^2 A_S(h)/h^2} \tag{A.5}$$

NOTE 1 The formula gives HM_S in MPa. To get HM_S in GPa a factor of 10^{-3} is required.

NOTE 2 $A_S(h) = 26{,}43 \times h^2$ for the Vickers indenter ($2\alpha = 136°$), $A_S(h) = 26{,}43 \times h^2$ for the original Berkovich indenter ($\alpha = 65{,}03°$) and $A_S(h) = 26{,}98 \times h^2$ for the modified Berkovich indenter ($\alpha = 65{,}27°$).

A.3.2 Designation of Martens hardness, HM_S

EXAMPLE

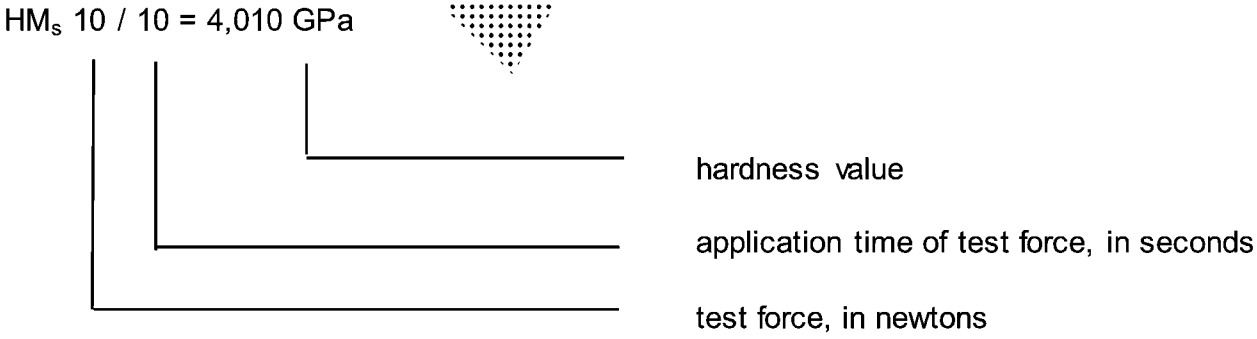

NOTE The method for determining Martens hardness from the slope of the increasing force/indentation depth curve has the advantage of being independent of the uncertainty of the determination of the zero-point and the test piece roughness. There is also a lower influence of vibration at the location of the testing machine on the test results. For test pieces exhibiting a variation in hardness as a function of indentation depth, the determined hardness values, HM_S, deviate from HM determined as in A.2.1. In this case, the concept of differential Martens hardness, HM_{diff}, as described in A.3.3, can be applied.

A.3.3 Determination of Martens hardness from the first derivative of the increasing force/indentation curve, HM_{diff}

The concept of the determination of the Martens hardness given by the slope of the increasing force/indentation depth curve can be extended to materials with variation in hardness as a function of indentation depth. A material with HM(h) = const. can be analysed with a linear regression of h vs. $F^{1/2}$ over a large portion of the force/indentation depth curve to obtain a single HM_S value (see A.3.1). When HM varies with h, stepwise linear regression can be performed over small portions of the curve.

In the limit for infinitesimal step widths, the first derivative of h vs. $F^{1/2}$ is calculated (local slope). Formula (A.5) can then be rewritten as Formula (A.6):

$$HM_{diff} = \frac{1}{\left(\frac{\partial h}{\partial \sqrt{F}}\right)^2 \frac{A_s}{h^2}} \tag{A.6}$$

where

A_s/h^2 is equal to 26,43 for the Vickers and orignal Berkovich indenters (see Note 1 in A.2.1).

NOTE The formula gives HM_{diff} in MPa. To get HM_{diff} in GPa a factor of 10^{-3} is required.

It is known that (numerical) differentiation increases the experimental noise of the curves, and this shall be included when calculating uncertainties.

For hardness profiles, a notation as for HM or HM_s is not possible, thus the differential Martens hardness should be reported as a graph of HM_{diff} vs. h or HM_{diff} vs. F. Any variation of HM_{diff} with depth shall be interpreted in the light of a complete understanding of the indentation size effect.

A.4 Indentation hardness

A.4.1 Determination of indentation hardness, H_{IT}

Indentation hardness H_{IT} is a measure of the resistance to permanent deformation or damage and, to a first approximation, is given in Formula (A.7).

$$H_{IT,0} = \frac{F_{max}}{A_p(h_c)} \tag{A.7}$$

where

F_{max} is the maximum applied force;

$A_p(h_c)$ is the projected (cross-sectional) area of contact between the indenter and the test piece.

NOTE 1 The formula gives $H_{IT,0}$ in MPa. To get $H_{IT,0}$ in GPa a factor of 10^{-3} is required.

NOTE 2 This definition is in accordance with that first proposed by Meyer.[3]

The contact depth, h_c, is derived from the force removal curve using the tangent depth, h_r, and the maximum indentation depth, h_{max}, correcting for elastic displacement of the surface according to Sneddon's analysis,[5] contained in Formula (A.8), where $\varepsilon(m)$ is a variable in the range $0,6 < \varepsilon < 0,8$ the value of which depends on the indenter geometry and the extent of plastic yield in the contact, for more information see Reference [13].

$$h_c = h_{max} - \varepsilon(m) \times (h_{max} - h_r) \tag{A.8}$$

where

$\varepsilon(m)$ is a variable in the range $0,6 < \varepsilon < 0,8$; the exact value depending on the indenter geometry and the extent of plastic yield in the contact and is calculated using Formula (A.11). For more information, see Reference [13];

h_r is the intercept with the displacement axis of the tangent to the force-removal curve at F_{max}.

Different methods have been used for the determination of h_r and can be essentially described by two approaches.

a) *Linear extrapolation method* (see Reference [10]): this assumes that the first portion of the unloading curve is linear and simply extrapolates that linear portion to intercept the displacement axis. The intercept of this tangent with the displacement axis yields h_r.

   This method is only recommended for use with highly plastic materials where the depth of elastic recovery is less than 10 % of h_{max}.

   NOTE 3 Often, the range between 98 % F_{max} and 80 % F_{max} is taken for the least-square fitting procedure.

   If a linear fit to the force removal curve is used, then the values for epsilon in Table A.1 shall be used.

b) *Power law method* (see Reference [4]): this recognizes the fact that the first portion of the removal curve of the test curve is generally not linear, but can be described by a simple power law relationship as given in Formula (A.9):

$$F = B \times (h - h_p)^m \tag{A.9}$$

where

B is a constant;

m is an exponent that depends on indenter geometry and contact plasticity.

B and m are determined by fitting the force removal data curve by the given power law relationship.

Often, the range between 98 % F_{max} and 20 % F_{max} is taken for the least-square fitting procedure, but this can be varied according to the "quality" of the unloading curve. If it is necessary to restrict the data fitted to less than the top 50 % of the force removal curve, the indentation experiment shall be considered to be abnormal and care should be taken in its interpretation. The tangent is found by differentiating the fitted power law relationship and evaluating at F_{max}. The intercept of this tangent with the displacement axis yields h_r.

If the exponent, m, exceeds certain values the resulting h_r should be interpreted very carefully. (For example: $m > 1{,}5$ is a sign that the results can have some time dependence. Values of $m > 2$ mean that the contact area would have to be sharper than the indenter, which is physically impossible, see Reference [16].)

The value of m obtained is then used to calculate $\varepsilon(m)$. This can be implemented by direct calculation using gamma functions Γ [Formula (A.10)] or by using a suitable approximation. One possible approximation (see Reference [13]) is Formula (A.11). The error introduced by using this approximation is less than 0,5 % for the range $1{,}05 \leq m \leq 5$.

$$\varepsilon(m) = m \cdot \frac{(h_{max} - h_c)}{h_{max}} = m \cdot \left[1 - \frac{1}{\sqrt{\pi}} \frac{\Gamma\left(\frac{m}{2m-2}\right)}{\Gamma\left(\frac{2m-1}{2m-2}\right)} \right] \tag{A.10}$$

$$\varepsilon(m) = \frac{0{,}08158}{\sqrt{m - 0{,}94}} - \frac{0{,}61679}{(m-0{,}94)^{0{,}02}} + \frac{1{,}26386}{(m-0{,}94)^{0{,}001}} \tag{A.11}$$

Other approximations are permitted such as the use of a look up table (see e.g. Reference [22]).

Table A.1 — Correction factor ε for different indenter geometries when using a linear fit

Indenter geometry	ε
Flat punch	1
Conical	$2(\pi - 2)/\pi = 0{,}73$

Table A.1 *(continued)*

Indenter geometry	ε
Paraboloid of revolution (includes spherical)	3/4
Berkovich, Vickers	3/4

For an indentation contact depth > 6 µm, a first approximation to the projected area, A_p, is given by the theoretical shape of the indenter [Formulae (A.12) and (A.13)].

a) Vickers indenter

$$H_{IT,0} = \frac{F_{max}}{A_p(h_c)} = 4{h_c}^2 \tan^2 \alpha \quad \text{(A.12)}$$

NOTE 4 The formula gives $H_{IT,0}$ in MPa. To get $H_{IT,0}$ in GPa a factor of 10^{-3} is required.

b) Berkovich indenter

$$H_{IT,0} = \frac{F_{max}}{A_p(h_c)} = 3 \cdot \sqrt{3} \cdot {h_c}^2 \tan^2 \alpha \quad \text{(A.13)}$$

NOTE 5 The formula gives $H_{IT,0}$ in MPa. To get $H_{IT,0}$ in GPa a factor of 10^{-3} is required.

where

h_c is the depth of contact of the indenter with the test piece calculated as in Formula (A.8).

The designation of angle α for Vickers and Berkovich geometry indenters is shown in Figure A.1.

NOTE 6 $A_p(h) = 24{,}50 \times h^2$ for the Vickers indenter ($2\alpha = 136°$), $A_p(h) = 23{,}97 \times h^2$ for the original Berkovich indenter ($\alpha = 65{,}03°$) and $A_p(h) = 24{,}49 \times h^2$ for the modified Berkovich indenter ($\alpha = 65{,}27°$).

NOTE 7 Most Berkovich indenters in use have, in fact, a modified Berkovich geometry.

NOTE 8 The maximum indentation depth, h_{max}, is the depth at maximum test force and measured at the start of force removal. It includes any additional creep displacement that has occurred in any hold periods up until force removal.

For an indentation contact depth < 6 µm, the area function of the indenter cannot be assumed to be that of the perfect theoretical shape, since all pointed indenters have some degree of rounding at the tip and spherically ended indenters (spherical and conical) are unlikely to have a uniform radius. The determination of the exact area function for a given indenter is required for indentation contact depths < 6 µm, but is also beneficial for larger indentation depths (see ISO 14577-2:2015, 4.5.1 and 4.6).

NOTE 9 The area function, $A_p(h)$, is normally expressed as a mathematical function relating the projected area of contact to the distance from the tip of the indenter. Where the area function cannot be described by a relatively simple (cubic or polynomial) mathematical function, then an estimate can be made either graphically or by using a look-up table. Alternatively, a different mathematical function can be used to describe different parts of the indenter or a spline function adopted.[21]

In all cases, the estimated hardness values H_{IT} shall be corrected for radial displacement of the surface using the method given in Annex I, to give the value of $H_{IT,n}$ (where n is the number of iterations used in the correction) using the estimated H_{IT} value as initial estimations $H_{IT,0}$. For more information, see Reference [13]. The radial correction is small for most metals (<0,5 %) but rises to 5 % for highly elastic materials such as fused silica.

Information concerning the correlation of H_{IT} to other hardness scales is contained in Annex F.

A.4.2 Designation of indentation hardness, H_{IT}

EXAMPLE

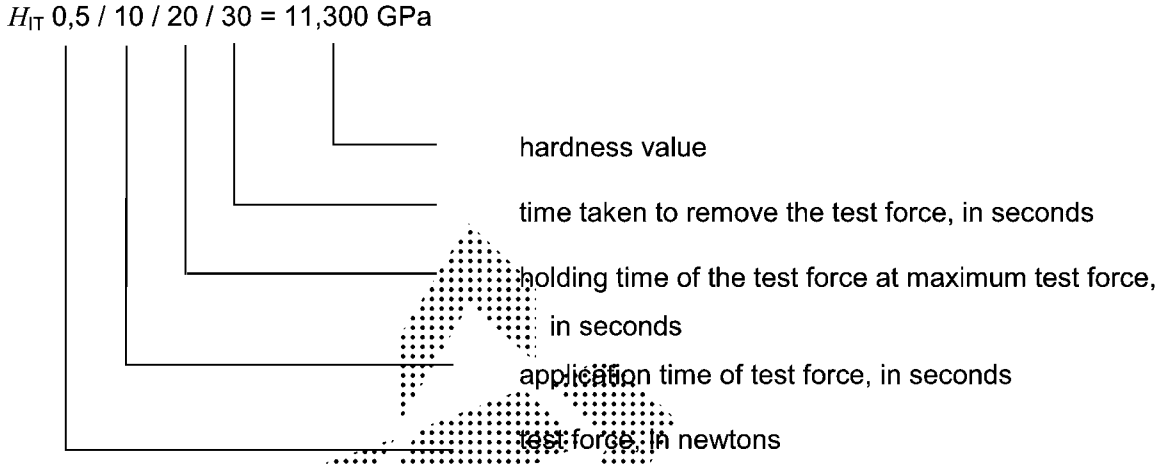

A.5 Indentation modulus

A.5.1 Determination of indentation modulus, E_{IT}

The force removal curve is fitted and the contact depth derived in the same way as in A.4.1. An initial estimate of the reduced modulus is calculated using Formula (A.14). This value shall then be corrected for radial displacement of the surface using the method given in Annex I to give the value of $E_{r,n}$ (where n is the number of iterations used in the correction) using the estimated E_r value as initial estimations $E_{r,0}$. For more information see Reference [13]. Using Formula (A.15), a value for the plane strain modulus, E^*, can be calculated. Using the Poisson's ratio of the test piece (known or estimated), the indentation modulus can be calculated using Formula (A.16) and is comparable with the Young's modulus of the material. However, significant differences between the indentation modulus, E_{IT}, and Young's modulus can occur, if either pile-up or sink-in is present.

$$E_{r,0} = \frac{\sqrt{\pi}}{2C_s\sqrt{A_p(h_c)}} \tag{A.14}$$

$$E^* = \frac{1}{\frac{1}{E_{r,n}} - \frac{1-(\nu_i{}^2)}{E_i}} = \frac{E_{IT}}{1-(\nu_s{}^2)} \tag{A.15}$$

$$E_{IT} = \frac{1-(\nu_s)^2}{\frac{1}{E_{r,n}} - \frac{1-(\nu_i)^2}{E_i}} \quad (A.16)$$

where

ν_s is the Poisson's ratio of the test piece;

ν_i is the Poisson's ratio of the indenter (for diamond 0,07) (e.g. in Reference [6]);

E_r is the reduced modulus of the indentation contact;

E_i is the modulus of the indenter (for diamond 1140 GPa) (e.g. in Reference [6]);

C_S is the compliance of the contact, i.e. dh/dF of the test force removal curve (corrected for machine compliance) evaluated at maximum test force (reciprocal of the contact stiffness);

A_p is the projected contact area, the value of the indenter area function at the contact depth, h_c, defined in accordance with ISO 14577-2:2015, 4.6.

For $h_c > 6$ µm, the following are valid:

$\sqrt{A_p}$ 4,950 × h_c for the Vickers indenter and the modified Berkovich indenter;

$\sqrt{A_p}$ is equal to 4,895 × h_c for the Berkovich indenter.

NOTE Formula (A.14) is based on an assumption of axis symmetric contact area. Corrections for pyramidal indenters have been proposed in Reference [14].

A variable epsilon (ε = 0,6 to 0,8) and radial displacement correction shall be used, see A.4.1. The method for estimation of radial displacement correction is given in Annex I. The radial correction is very small for most metals (<0,5 %) but reaches up to 5 % for highly elastic materials such as fused silica.

A.5.2 Designation of plane strain modulus, E^*, and indentation modulus, E_{IT}

EXAMPLE 1

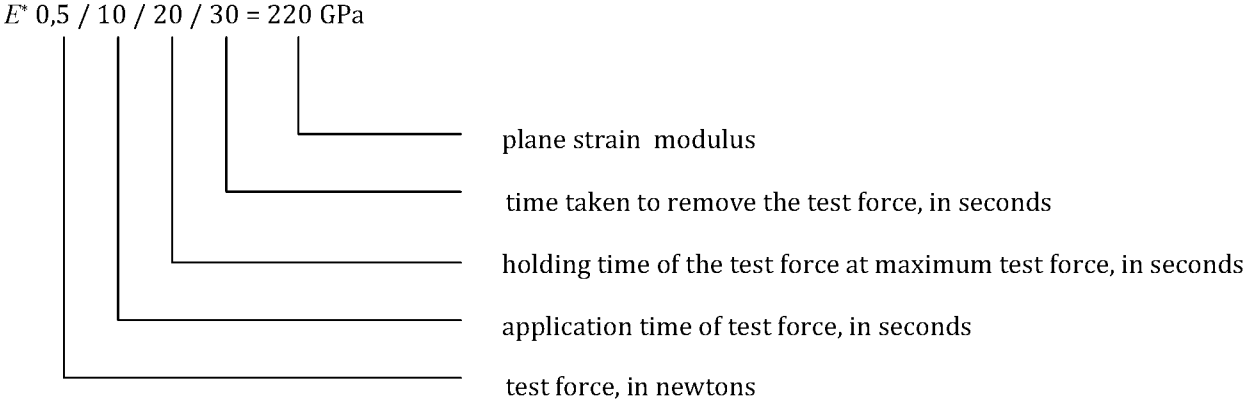

EXAMPLE 2

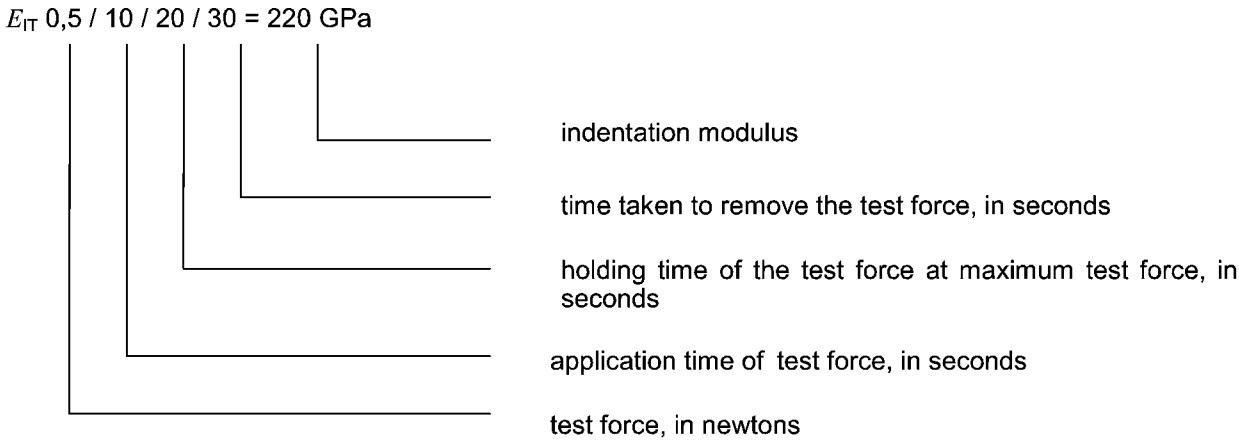

If the indentation modulus is given, then the value of the Poisson's ratio used for calculation shall be reported.

NOTE For some materials, a correlation between E_{IT} and tabular values for the Young's modulus of metals and metal alloys is demonstrated; see References [7] and [8].

A.6 Indentation creep

A.6.1 Determination of indentation creep, C_{IT}

If the change of the indentation depth is measured with constant test force, a relative change of the indentation depth can be calculated as given in Formula (A.17). This is a value for the creep of the material [see Figure B.1 a), Figure B.1 b), and Figure A.3].

$$C_{IT} = \frac{h_2 - h_1}{h_1} \times 100 \qquad \text{(A.17)}$$

where

h_1 is the indentation depth at the time (t_1) of reaching the test force, which is kept constant;

h_2 is the indentation depth at time (t_2) of holding the constant test force.

NOTE 1 While using Formula (A.17), C_{IT} is given as a percentage.

NOTE 2 The creep data can be significantly influenced by thermal drift.

A.6.2 Designation of indentation creep, C_{IT}

The relative change of the indentation depth (creep) is denoted by the symbol C_{IT}

EXAMPLE

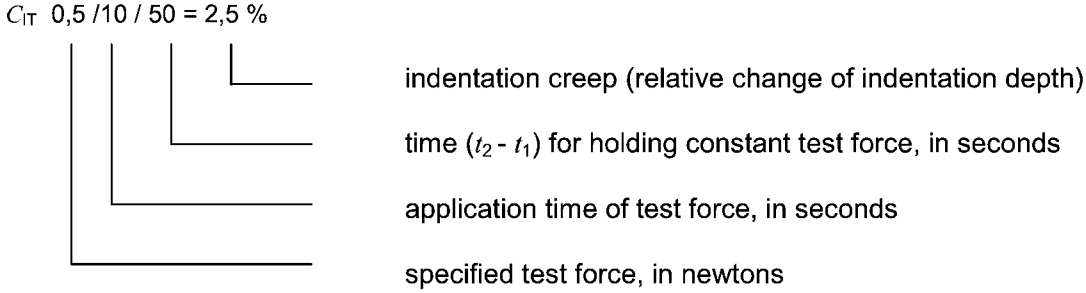

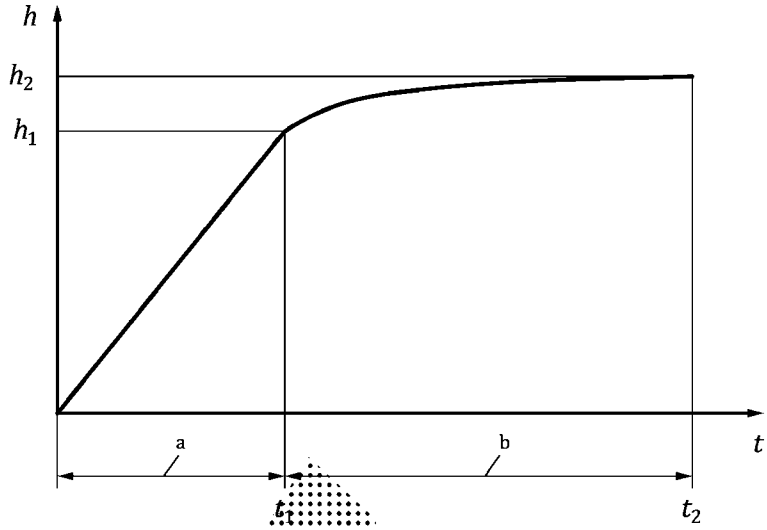

Key

a application of the test force

b test force kept constant from t_1 to t_2

Figure A.3 — Expression of indentation creep

A.7 Indentation relaxation

A.7.1 Determination of indentation relaxation, R_{IT}

If the change of the test force is measured at a constant indentation depth a relative change of the test force can be calculated as given in Formula (A.18). This is a value for the relaxation of the material [see Figure B.2 a), Figure B.2 b), and Figure A.4].

$$R_{IT} = \frac{F_1 - F_2}{F_1} \times 100 \qquad \text{(A.18)}$$

where

F_1 is the force at reaching the indentation depth, which was kept constant;

F_2 is the force after the time during which the indentation depth was kept constant.

NOTE For Formula (A.18), R_{IT} is given as a percentage.

A.7.2 Designation of indentation relaxation

The relative change of test force (relaxation) is denoted by the symbol R_{IT}.

EXAMPLE

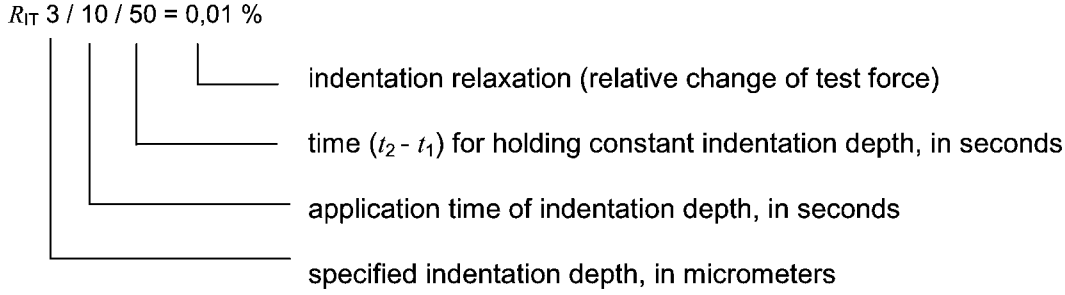

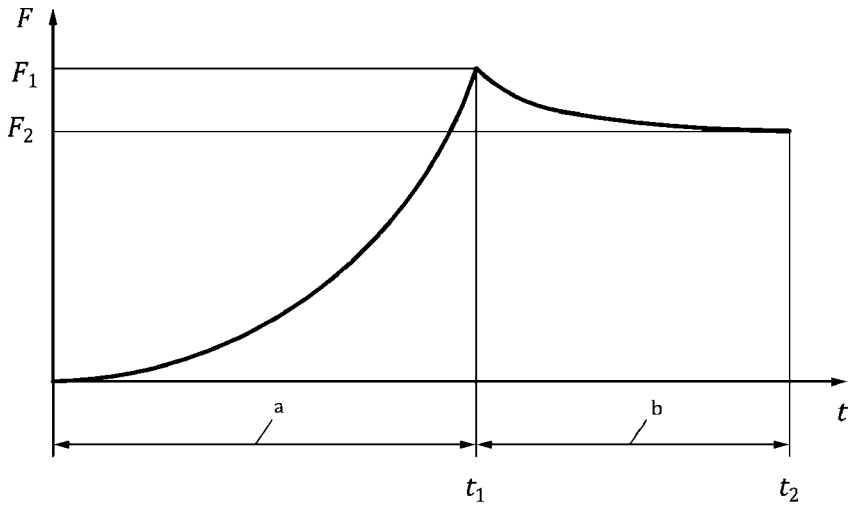

Key

a application of the indentation depth

b indentation depth kept constant from t_1 to t_2

Figure A.4 — Expression of indentation relaxation

A.8 Plastic and elastic parts of the indentation work

A.8.1 Determination of plastic and elastic parts of the indentation work

The mechanical work, W_{total}, indicated during the force application of the indentation procedure is only partly consumed as plastic deformation work, W_{plast}. During the removal of the test force, the remaining part is set free as work of the elastic reverse deformation, W_{elast}. According to the definition of the mechanical work as $W = \int F \mathrm{d}h$, both parts appear as different areas in Figure A.5. Formula (A.19) contains information which is suitable for characterization of the test piece.

$$\eta_{IT} = \frac{W_{elast}}{W_{total}} \times 100 \tag{A.19}$$

where

$$W_{total} = W_{elast} + W_{plast} \tag{A.20}$$

NOTE For Formula (A.20), η_{IT} is given as a percentage.

The plastic part is calculated as given in Formula (A.21):

$$W_{plast} / W_{total} = 100\,\% - \eta_{IT} \tag{A.21}$$

If the mechanical work is not calculated by integration of the recorded indentation curve, the specific type of procedure, for instance the use of fitted curves, shall be reported.

A.8.2 Designation of elastic part of indentation work, η_{IT}

EXAMPLE

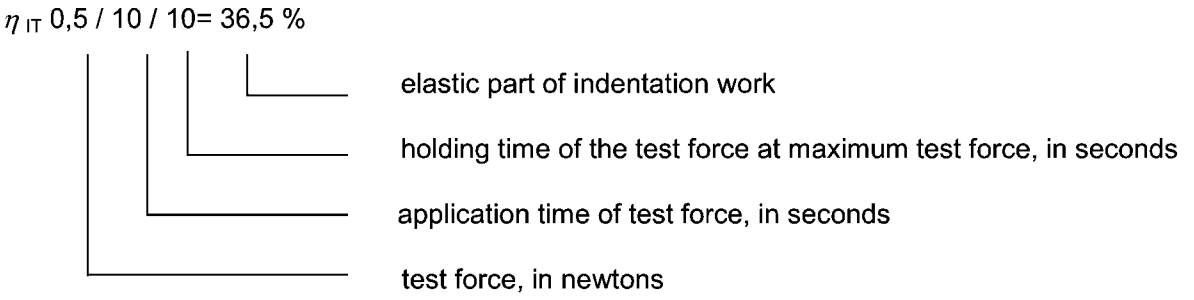

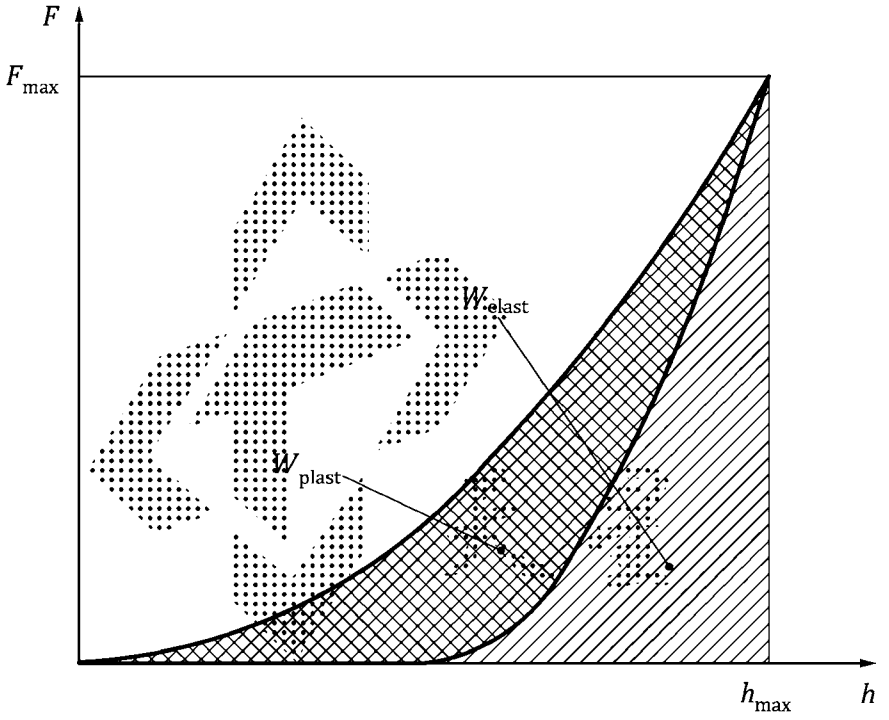

Figure A.5 — Plastic and elastic parts of the indentation work

Annex B
(informative)

Types of control use for the indentation process

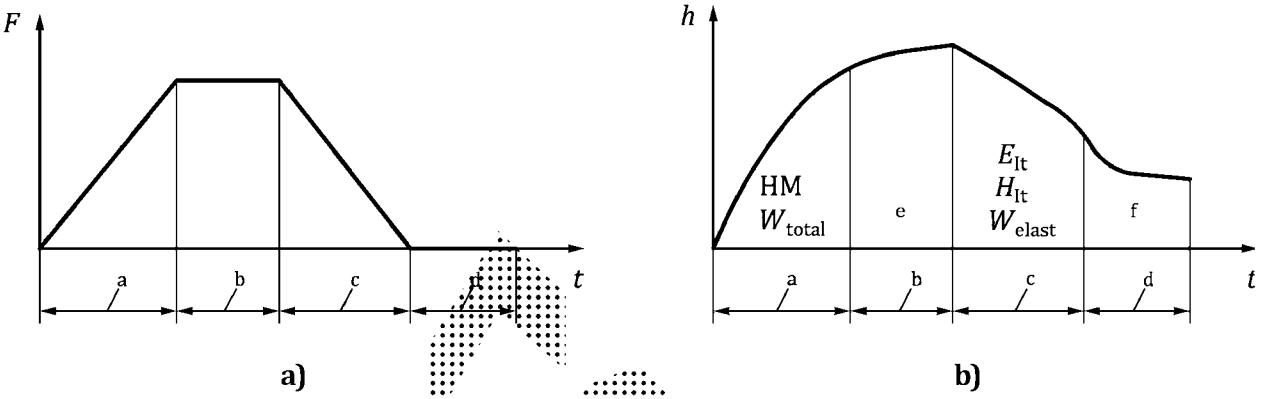

a) b)

Key

a	application of test force	d	test force = 0 N
b	maximum test force	e	indentation creep
c	removal of test force	f	recovery at zero test force

Figure B.1 — Schematic representation of the test force controlled test procedure in dependence on time

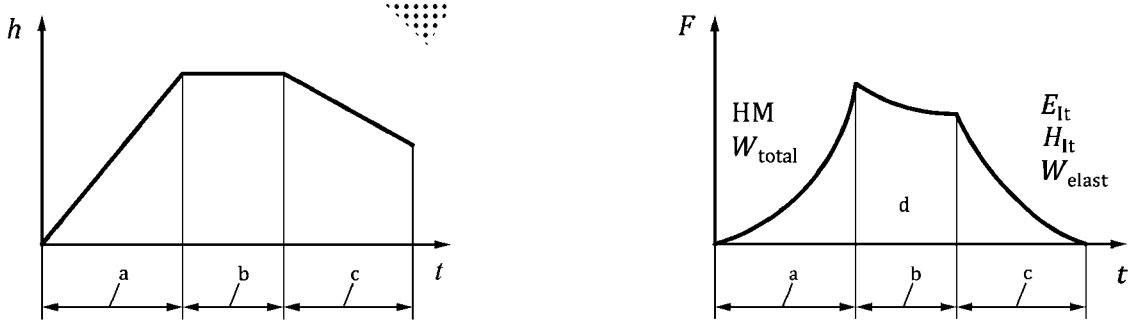

a) b)

Key

a	application of indentation depth	c	decreasing of indentation depth
b	maximum indentation depth	d	relaxation under maximum indentation depth

Figure B.2 — Schematic representation of the indentation depth controlled test procedure in dependence on time

Annex C
(normative)

Machine compliance and indenter area function

C.1 Machine compliance

The applied test force acts not only on the test piece surface but also on the parts of the testing machine, which are elastically deformed.

This elastic deformation causes an increase in the measured indentation depth that is not experienced at the indentation contact, but occurs between the reference planes in the testing machine.

Usually, the additional indentation depth due to the test machine deformation is proportional to applied force. This additional compliance shall be taken into account at all forces when indentation modulus E_{IT}, Martens hardness HM, indentation hardness H_{IT}, and indentation work, e.g. η_{IT}, are being measured as it acts directly to increase h_{max} and decrease the gradient of the tangent to the removal curve of the test force. The increase in the measured value of h_{max} is especially significant at high applied forces.

The machine compliance can influence the test results, especially if the displacement measurement is bottom referenced. Procedures for the determination of the machine compliance are given in ISO 14577-2:2015, 4.4 and in References [10] and [12].

C.2 Indenter area function

The calculation of the material parameters described in A.2, A.3, A.4, and A.5 is based on the contact area (or projected area) of the indenter. However, only the indentation depth is measured. Crucial differences can be found when comparing the actual contact area with the area calculated assuming ideal (perfect) indenter geometry, particularly at small measured indentation depths.

These differences are due to the rounding of the tip of the indenter: in the case of the Vickers pyramid, the line of conjunction (offset) and the deviation from the specified angle of the indenter, which are attributable to the usual production tolerances. Furthermore, the actual contact area changes due to wear of the indenter tip.

To maintain the reproducibility of the results, it is necessary to determine the actual contact area (or projected area) and use it in the calculation of the materials parameters.

Two methods of determining the projected area function are possible, such as

— direct measurement using a traceable atomic force microscope (AFM); see Reference [11], and

— indirectly, by utilizing indentations into a material of known Young's modulus and Poisson's ratio (see Reference [12]) or known plane strain modulus.

Two methods of determining the surface area function are possible, such as

— direct measurement using a traceable atomic force microscope (AFM); see Reference [11], and

— indirectly, by utilizing indentations into a reference material of known and depth-independent Martens hardness and if there is some experimental evidence that, for the reference material being used under the given experimental conditions, the indentation size effect can be neglected.

For the indirect methods, machine compliance should first be determined and the indentation depth data should be corrected accordingly.

To ensure that indentation derived measurements of indenter projected area function agree between reference materials of different properties and with direct measurements (e.g. by AFM), a variable epsilon and radial displacement correction shall be used, see A.4.1. The method for estimation of radial displacement correction is given in Annex I. The radial correction is small for most metals (<0,5 %) but reaches up to 5 % for highly elastic materials such as fused silica.

NOTE 1 Indentation area function and machine compliance correction can be determined simultaneously using an iterative procedure and multiple reference materials together with a variable epsilon and the radial displacement correction; see References [12] and [13].

NOTE 2 The area function is normally expressed as a mathematical function relating the projected surface area to the distance from the tip of the indenter. Where the area function cannot be described by a relatively simple (cubic or polynomial) mathematical function, then an estimate can be made either graphically or by using a look-up table. Alternatively, a different mathematical function can be used to describe different parts of the indenter or a spline function adopted. (Public domain software exists for fitting splines or higher polynomials. [21]) A procedure for the verification of the indenter area function is given in ISO 14577-2:—, Annex B.

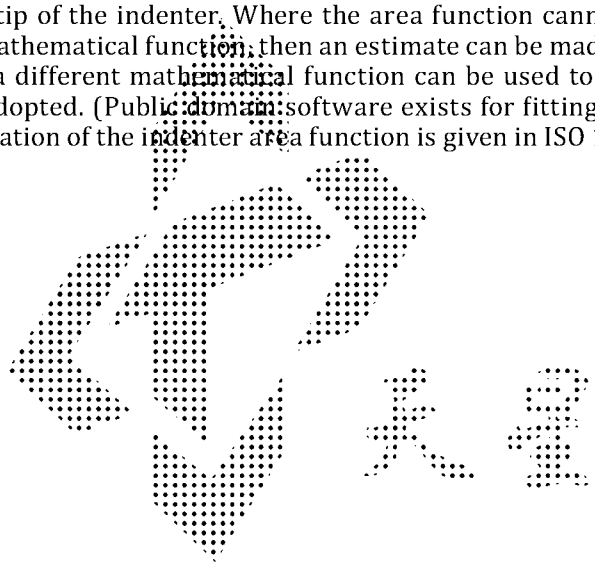

Annex D
(informative)

Notes on diamond indenters

D.1 Experience has shown that a number of initially satisfactory indenters can become defective after a comparatively short time in use. This is due to small cracks, pits or other flaws in the surface. If such faults are detected in time, many indenters can be reclaimed by regrinding. If not, any small defects on the surface rapidly worsen and make the indenter useless.

Therefore, the following apply.

— The condition of indenters should be monitored regularly for contamination or defects. For macro range indenters, this can be achieved by inspection of the shape of an indentation into a reference block or routine test material as used in ISO 14577-2:2015, 6.3.

— For micro and nano range indenters, periodic optical inspection using a 400 × microscope is recommended for detection of contamination and gross defects.

— Detection of sub-microscopic damage or contamination is possible by maintaining a good history or indirect verification and routine checking as given in ISO 14577-2:2015, 6.2 and 6.3, or by scanned probe microscopy of indentations or the indenter itself.

— The calibration certificate of the indenter is no longer valid when the indenter shows defects or after it is reground or otherwise repaired.

D.2 Contamination of the surface of the indenter can distort the test result. The source of contamination is most often testing on contaminated test pieces.

For micro and nano range indenters, the cleaning procedure could be as follows.

— Hold the indenter firmly and indent into a freshly cleaved surface of expanded polystyrene several times. The plasticizers make a good solvent and the foam-like nature is unlikely to damage the tip of the diamond. Inspect using an optical microscope at 400 × or greater and indent gently into a small cotton wool ball soaked in acetone or water-free alcohol (e.g. ethanol or iso-propanol) until there is no visible contamination.

— If the contamination is not removed by repeating the process above, an indentation into either aluminium, glass or the "end-grain" of a clean wooden spatula can dislodge the contamination sufficiently for removal using the above cleaning procedure.

— Care should be taken not to subject the indenter to excessive normal, and in particular lateral, forces during the indentations as this can damage the indenter. One method is to use a sample that weighs less than the usual forces experienced by the indenter and gently and slowly lower the sample on to the upturned indenter, thereby limiting the maximum force to that of the sample weight.

— An indentation with the maximum test force of the microindenter into PMMA and subsequent inspection of the indent at typically 400 × magnitude is also suitable to check the indenter for contaminations and damages.

Annex E
(normative)

Influence of the test piece surface roughness on the accuracy of the results

This annex is based on round-robin tests with Vickers indenters; see Reference [9].

Surface roughness causes an uncertainty in contact area due to asperity contact at very shallow indentation depths. At larger indentation depths, the uncertainty in contact area is reduced and is most conveniently expressed as an uncertainty in indentation depth proportional to the arithmetic (mean deviation) surface roughness.

To maintain the contribution of surface roughness to the uncertainty in indentation depth below 5 %, h shall be at least 20 × the arithmetic mean deviation roughness, Ra, as given by Formula (E.1); see ISO 4287.

$$h \geq 20\,Ra \tag{E.1}$$

Table E.1 gives examples for permissible surface roughness for different materials at different test forces.

Table E.1 — Examples for maximum permissible arithmetic surface roughness, *Ra*, for different test forces, *F*

Examples of materials	Maximum permissible arithmetic surface roughness, *Ra*			Martens hardness
	µm			HM
	0,1 N	2 N	100 N	N/mm²
aluminium	0,13	0,55	4,00	600
steel	0,08	0,30	2,20	2 000
hardmetal	0,03	0,10	0,80	15 000

NOTE Interlaboratory tests (see Reference [9]) show that the standard deviation, s_h, of the indentation depth is approximately equal to the arithmetic roughness, Ra. The requirement for uncertainty of $h < 5$ % leads to the minimum indentation depth.

For tests at the nano and lower limit of the micro range, it might not be possible to meet the condition of Formula (E.1) for higher hardness test pieces. To reduce the uncertainty in the mean value of the test result, the number of tests can be increased. This should be stated in the test report.

It is recommended for tests in the nano and micro ranges that surface roughness of the indented contact area be measured or that this area be observed by suitable means. In many cases, surface roughness can be inferred from comparison with test pieces of known roughness or from batch sampling of surface roughness. A visual inspection verifying a smooth, polished, or "mirror" finish is adequate for tests in the macro range. A known "mirror" finish metallographic preparation is adequate down to the lower micro range.

Annex F
(informative)

Correlation of indentation hardness H_{IT} to Vickers hardness

Indentation hardness, H_{IT}, can be correlated to Vickers hardness, HV, for a wide range of materials by using a suitable scaling function.

WARNING — Although H_{IT} can be correlated to HV in this way, any equivalent HV value so calculated should not be used as a substitute for HV.

A simple function can be derived for a perfect Vickers geometry indenter or for a Vickers indenter where the projected area function is known. In this case, measurements of the hardness, H_{IT}, expressed in GPa, is related to the Vickers hardness numbers, HV, expressed in kgf/mm^2, by a scaling factor.

The ratio of projected area, A_p, to surface area, A_s, at any particular distance from the tip of a perfect Vickers indenter, is a constant as given in Formula (F.1):

$$\frac{A_p}{A_s} = \frac{24{,}50}{26{,}43} = 0{,}926\,9 \tag{F.1}$$

The conventional Vickers hardness HV according to ISO 6507-1 is related to A_s

$$HV = \frac{1}{g_n} \times \frac{F}{A_s} \tag{F.2}$$

where

g_n is acceleration due to gravity, typically 9,806 65 m/s^2, thus

$$HV = \frac{1}{g_n} \times \frac{A_p}{A_s} \times \frac{F}{A_p} = 10^3 \times \frac{1}{g_n} \times \frac{A_p}{A_s} \times H_{IT} = 94{,}53 H_{IT} \tag{F.3}$$

For an original Berkovich indenter, the relationship in Formula (F.4) holds:

$$\frac{A_p}{A_s} = \frac{23{,}96}{26{,}43} = 0{,}906\,5 \tag{F.4}$$

Thus, HV, expressed in kgf/mm^2, can be expressed in terms of H_{IT}, expressed in GPa, as given in Formula (F.5):

$$HV = \frac{1}{g_n} \times \frac{A_p}{A_s} \times \frac{F}{A_p} = 10^3 \times \frac{1}{g_n} \times \frac{A_p}{A_s} \times H_{IT} = 92{,}44 H_{IT} \tag{F.5}$$

For a modified Berkovich indenter, the relationship in Formula (F.6) holds:

$$\frac{A_p}{A_s} = \frac{24,50}{26,97} = 0,9083 \tag{F.6}$$

Thus, HV, expressed in kgf/mm^2, can be expressed in terms of H_{IT}, expressed in GPa, as given in Formula (F.7):

$$\mathrm{HV} = \frac{1}{g_n} \times \frac{A_p}{A_s} \times \frac{F}{A_p} = 10^3 \times \frac{1}{g_n} \times \frac{A_p}{A_s} \times H_{IT} = 92,62 H_{IT} \tag{F.7}$$

Be aware that perfect indenter geometry is generally not maintained for small indentation depths (<6 µm) and, therefore, this simple correlation can break down. The error induced by such an assumption is, in general, most severe at small indentation depths.

For some materials, a correlation between H_{IT} 1/10/20/30 and HV 0,1 is demonstrated; see References [4] and [7].

Annex G
(normative)

Drift and creep rate determination

G.1 Instrument drift

A decision tree to assist in estimating the drift during the experiment is shown in Figure 3. If the drift rate is significant, the displacement data shall be corrected by measuring the drift rate during a hold at an applied force as close to zero force as is practicable or during a hold at a suitable place in the force removal curve. If a fully elastic contact can be obtained, a hold at initial contact is preferred. The hold period shall be sufficient to allow determination of the average displacement drift rate due to the instrument (e.g. due to temperature changes) and a linear correction shall be applied to all measured displacement values. The drift rate correction obtained in this way is valid only if the drift (as opposed to noise) in the displacement values determined during the hold period (wherever it is in the indentation cycle) is believed to result from purely instrumental effects (such as temperature) and not from indentation-induced responses from the material (e.g. visco-elastic or inelastic creep, fracture, pressure induced phase transformations, etc.). If material influences cannot be avoided, drift rates shall be measured before and after each indentation (e.g. using an elastic contact with a hard reference surface). Either the average linear drift rate can be calculated or the drift rate linearly interpolated over the time between the two measurements.

If a purely elastic contact cannot be obtained, there is no generally recommendable method. Depending on the material under investigation, a hold at a near zero initial force or at up to 90 % removed force (e.g. soft material) might be preferred. Because of the stiffer contact (higher contact area) in the force removal curve, dispersion of the data when using this method is generally lower. For difficult materials, a hold period at both ends of the indentation cycle can be included. It is recommended that the hold period be for at least the force application time and the first 10 s to 20 s of the hold data should be discarded in the calculation of drift rate, since these initial data can be significantly influenced by time-dependent effects (stage settling, material time-dependent deformation, formation of capillary surface layers etc.), see Reference [15].

G.2 Contact creep rate at F_{max}

A further hold period shall be performed at maximum force to allow for completion of any time-dependent deformation. The minimum hold period length is, therefore, dependent on the instrument capability and the material being tested. The hold period shall be long enough and/or the time to remove force shall be short enough such that the relationship in Formula (G.1) holds:

$$q_F > 10 \cdot \frac{q_c}{C_T} \tag{G.1}$$

where

q_F is the force removal rate;

q_c is the contact creep rate at F_{max};

C_T is the measured compliance (dh/dF) at (F_{max}, h_{max}).

The creep rate is defined as the linear fit to the displacement vs. time for the last 30 data points before force removal begins.

NOTE 1 The error in measured compliance, b_C, (due to the creep rate at the point of force removal), expressed as a percentage, depends on the range of force removal data fitted, the fit algorithm used, the absolute contact compliance and the rate of force removal. An estimate of the worst-case error b_c in the measured contact compliance can be calculated using Formula (G.2):

$$b_C = \sqrt{10^{-3}} \times \frac{q_C}{\left(\frac{\sqrt{\pi}}{2} \cdot \frac{\sqrt{H_{IT}}}{E_r} \cdot \frac{1}{\sqrt{F_{max}}}\right) \cdot \left(\frac{dF}{dt}\right)} \times 100 \qquad \text{(G.2)}$$

The hardness (and modulus) can be depth-dependent, particularly if a non-self-similar indenter is used.

NOTE 2 When visco-elastic materials are tested, the drift rate does not necessarily decrease by increasing the hold at maximum force. Even if it does, the drift rate will reverse when the force is removed as visco-elastic recovery begins. The practice of using a measurement of creep rate just before force removal to apply a creep rate correction to the force removal data are not recommended. The elastic modulus of visco-elastic materials is better tested using an indentation cycle faster than the visco-elastic time constant or by using dynamic (ac) indentation methods.

Force application and removal rates can be the same, but it is recommended that the removal rate should be higher than the application rate (if possible) to minimize the influence of creep. Slower force application reduces the hold period length required at F_{max} to achieve the necessary reduction in creep rate.

NOTE 3 The influence of material creep behaviour on hardness and modulus results has been reported; see Reference [15]. The results show that, especially for materials with low hardness-to-modulus ratio (which includes most metals), the modulus results are not reliable if the hold period is too short. A modulus error, due to creep, of more than 50 % can arise. The variation of the hold period produced a hardness change of up to 18 %. Reference [15] proposes hold periods dependent on the material type that range from 8 s for fused quartz to 187 s for aluminium. The criterion used was that the creep rate should have decayed to a value where the depth increase in 1 min is less than 1 % of the indentation depth. It should be noted that creep of 1 % of the total indentation depth can cause a large change in the apparent contact stiffness in nearly perfectly plastic materials such as metals.

It is recommended that the creep rate be assessed in preliminary experiments. The force removal rate should be the highest possible that still ensures sufficient force removal data for the subsequent analysis.

Annex H
(informative)

Estimation of uncertainty of the calculated values of hardness and materials parameters

H.1 General remarks

Measurement uncertainty analysis is a useful tool to help determine sources of error and to understand differences in test results. This annex gives guidance on uncertainty estimation but the values derived are for information only.

H.2 Procedures

H.2.1 General

In this annex, two methods for the estimation of uncertainty of calculated hardness and materials parameters are described.

Method 1: This approach for determining uncertainty considers only those uncertainties associated with the overall measurement performance of the testing machine with respect to the reference blocks (abbreviated as CRM below). These performance uncertainties reflect the combined effect of all the separate uncertainties (indirect verification). Because of this approach, it is important that the individual machine components are operating within the tolerances and all tests conducted according to this part of ISO 14577. The underlying assumption of this method is that all of the uncertainties experienced by the test are the same when indenting a CRM. This might not be true if there are differences in indentation cycles used or the CRM material properties are different from the test piece or if the indentations are of different sizes, resulting in significant indentation size effects.

Method 2: This approach considers a complete quantification of all the identified contributions to the uncertainty (see Clause 8).

H.2.2 Method 1

Different machines will produce different deviations (bias or error) b (see Table H.1, step 6) to the certified value of a reference block. It can be expected that this is a constant and systematic effect for a particular machine. It is also expected that this bias is large with respect to the random components of uncertainty and therefore is dominant. The expanded uncertainty U is therefore given by Formula (H.1) and the result by Formula (H.2) (see Table H.1 steps 8 and 9)

$$U = k \cdot \sqrt{u_{\mathrm{CRM}}^2 + u_{\mathrm{HM}}^2 + u_x^2} + |b| \tag{H.1}$$

$$\overline{X} = \overline{x} \pm U \tag{H.2}$$

In ISO/IEC Guide 98-3, it is recommended to correct the mean value to compensate for known systematic effects. To do this it is necessary that all determined values be corrected by b (This assumes that the bias in testing the reference block will be exactly the same when testing the test piece). If the mean value is corrected by the bias, then it is no longer an uncertainty itself. However, the (smaller) uncertainty, u_{b},

in determined value of b is an additional contribution to the uncertainty of the corrected results. The uncertainty of the corrected value, U_{corr}, is then given by Formula H.3 (see Table H.1 steps 10 and 11)

$$U_{corr} = k \cdot \sqrt{u_{CRM}^2 + u_{HM}^2 + u_{\bar{x}}^2 + u_b^2} \quad \text{(H.3)}$$

When the result is corrected for the bias, the result of the measurement is given by Formula (H.4):

$$\bar{X}_{corr} = (\bar{x} + \bar{b}) \pm U_{corr} \quad \text{(H.4)}$$

Table H.1 — Determination of the corrected expanded uncertainty e.g. for Martens hardness

Step	Sources of uncertainty	Symbol	Formula	Comments	Example of HM GPa
1	Standard uncertainty and mean value of Martens hardness of CRM	u_{CRM}, $\bar{X}_{CRM}$	$u_{CRM} = \frac{U_{CRM}}{2}$	U_{CRM}, $\bar{X}_{CRM}$ according to calibration certificate of CRM	$u_{CRM} = \frac{0{,}161}{2}$ $= 0{,}081$ $\bar{X}_{CRM} = 4{,}042$
2	Mean value and standard deviation when measuring the CRM using the test instrument	$\overline{HM}$ s_{HM}	$\overline{HM} = \frac{\sum_{i=1}^{n} H_i}{n}$ $s_{HM} = \sqrt{\frac{1}{n-1}\sum_{i=1}^{n}(H_i - \overline{HM})^2}$	$n = 5$ 5 measurements on the CRM	Single values 4,13; 4,14; 4,18; 4,13; 4,15 $\overline{HM} = 4{,}146$ $s_{HM} = 0{,}021$
3	Standard uncertainty of the mean value obtained by the testing machine when measuring the CRM piece	$u_{\overline{HM}}$	$u_{\overline{HM}} = \frac{t \cdot s_{HM}}{\sqrt{n}}$	$t = 1{,}14$ for $n = 5$	$u_{\overline{HM}} = \frac{1{,}14 \times 0{,}021}{\sqrt{5}}$ $= 0{,}011$
4	Mean value and standard deviation when measuring the test piece	$\bar{x}$ s_x	$\bar{x} = \frac{\sum_{i=1}^{n} x_i}{n}$ $s_x = \sqrt{\frac{1}{n-1}\sum_{i=1}^{n}(x_i - \bar{x})^2}$	$n = 5$ 5 measurements on the test piece	Single values 6,56; 6,65; 6,63; 6,42; 6,40 $\bar{x} = 6{,}532$ $s_x = 0{,}116$
5	Standard uncertainty of the mean value obtained by the testing machine when measuring the test piece	$u_{\bar{x}}$	$u_{\bar{x}} = \frac{t \cdot s_x}{\sqrt{n}}$	$t = 1{,}14$ for $n = 5$	$u_{\bar{x}} = \frac{1{,}14 \times 0{,}116}{\sqrt{5}}$ $= 0{,}059$
6	Deviation of hardness testing machine from calibration value for different measurement series	b	$b = \overline{HM} - \bar{X}_{CRM}$	difference between mean value and certified values	$b = 4{,}146 - 4{,}042 = 0{,}104$
7	Standard uncertainty of the determination of b is the RSS of the uncertainties in measuring the CRM and the CRM certification	u_b	$u_b^2 = u_{\overline{HM}}^2 + u_{CRM}^2$	if u_b is greater than b then no correction is necessary	$u_b = \sqrt{0{,}011^2 + 0{,}081^2} = 0{,}0817$
8	Determination of the expanded uncertainty	U	$U = k \cdot \sqrt{u_{CRM}^2 + u_{\overline{HM}}^2 + u_{\bar{x}}^2} + \lvert b \rvert$	$k = 2$	$U = 2 \cdot \sqrt{0{,}081^2 + 0{,}011^2 + 0{,}059^2}_{+0{,}104}$ $= 0{,}306$
9	Result of measurement	$\bar{\bar{X}}$	$\bar{\bar{X}} = \bar{x} \pm U$	—	$\bar{\bar{X}} = 6{,}532 \pm 0{,}306$

Table H.1 *(continued)*

Step	Sources of uncertainty	Symbol	Formula	Comments	Example of HM GPa
10	Determination of the corrected expanded uncertainty	U_{corr}	$U_{\text{corr}} = k \cdot \sqrt{u_{\text{CRM}}^2 + u_{\text{HM}}^2 + u_{\bar{x}}^2 + u_b^2}$	$k = 2$	$U_{\text{corr}} = 2 \cdot \sqrt{0{,}081^2 + 0{,}011^2 + 0{,}059^2 + 0{,}0817^2} = 0{,}26$
11	Result of the measurement with corrected mean value	$\bar{X}_{\text{corr}}$	$\bar{X}_{\text{corr}} = (\bar{x} - b) \pm U_{\text{corr}}$	—	$\bar{X}_{\text{corr}} = (6{,}532 - 0{,}104) \pm 0{,}26$

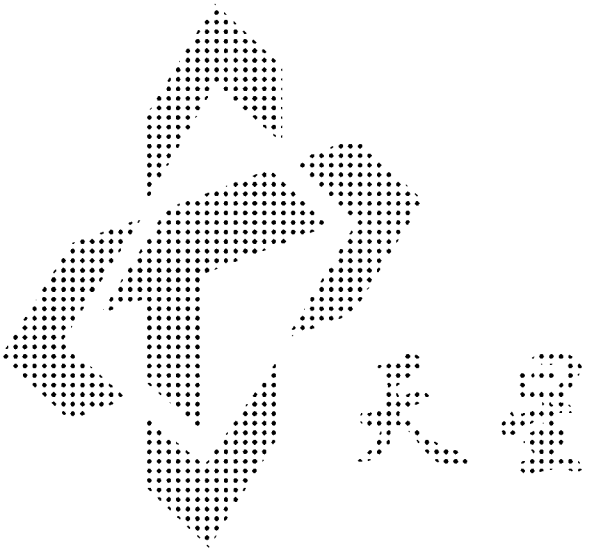

H.2.3 Method 2

H.2.3.1 General

H.2.3.1.1 This approach considers a complete quantification of all identified contributions to the random uncertainty (see Clause 8).

H.2.3.1.2 The user requires the following calibration uncertainties:

— displacement calibration (possibly expressed as a function of depth);

— force calibration;

— machine compliance calibration (possibly a function of force);

— area function calibration (probably expressed as a function of depth).

H.2.3.1.3 It is assumed that the above calibration uncertainties are available and can be expressed as a standard error at the particular depth and force for the data being analysed. It is also assumed that the force-displacement data have been corrected for the effects of thermal drift rate and instrument frame compliance, so that there are no systematic errors from these effects to include in the total uncertainty budget, only random errors in the values used for the corrections.

H.2.3.1.4 The above calibrations can be obtained in a variety of ways, each with their own set of uncertainties, which will have been calculated and combined by the accredited calibration laboratory performing them.

H.2.3.1.5 It is anticipated that the user is able to use the same data for calculating uncertainties as was used to obtain the values for hardness or modulus being reported. A typical indentation cycle, which includes all of the required elements

— approaches to contact,

— holds at contact force to obtain thermal drift and vibration data,

— increases force to F_{max} at test rate,

— holds at F_{max} to obtain creep rate,

— removes force (90 %) (optional hold for thermal drift/vibration measurement), and

— removes 100 % force.

H.2.3.1.6 The user shall then use the data itself to correct for thermal drift and calculate the following measurement uncertainties, which are unique to the particular data being analysed:

— uncertainty (standard deviation) in maximum indentation depth;

— uncertainty (standard deviation) in force removal slope;

— uncertainty in zero point assignation (For feedback controlled approaches, this can be the displacement step size at the assigned zero point. For zero points assigned by back extrapolation from the contact force, the standard error in the extrapolation intercept can be used.);

— residual drift rate (creep) at commencement of force removal.

NOTE The first two uncertainty measurements conveniently combine a great number of individual uncertainties, for which it would be difficult and expensive to obtain individual values. These include effects due to the actual sample being tested; such as the effect of surface roughness and/or contamination etc. It is, therefore, a very poor estimate to use historical data to estimate these uncertainty contributions. The most accurate estimates of the total uncertainty are, therefore, calculated using the values from a large number of replicate experiments. Estimates of the standard deviation of force removal slope and maximum indentation depth are not possible at all for a single measurement and suffer from a large uncertainty if small numbers of replicate indentations are analysed. It is recommended to use the same number of replicate experiments as suggested in ISO 14577-2:2015 (i.e. 10 or 15).

H.2.3.2 Modulus analysis

Using Formula (H.6) an uncertainty budget for E_r can be calculated.

$$E_r = \frac{\sqrt{\pi}}{2}\frac{1}{C_s\sqrt{A_p(h_c)}} = \frac{\sqrt{\pi}}{2}\frac{1}{\sqrt{A_p(h_c)}\times(C_T - C_F)} \tag{H.6}$$

where

C_T is the total compliance;

C_F is the frame compliance.

NOTE To obtain the uncertainty of the sample indentation modulus, E_{IT}, it requires the input of values for the diamond modulus and both diamond and sample Poisson's ratio and values for their uncertainties.

The breakdown of the uncertainty components for A_p and $(C_T - C_F)$ is shown in Figure H.1.

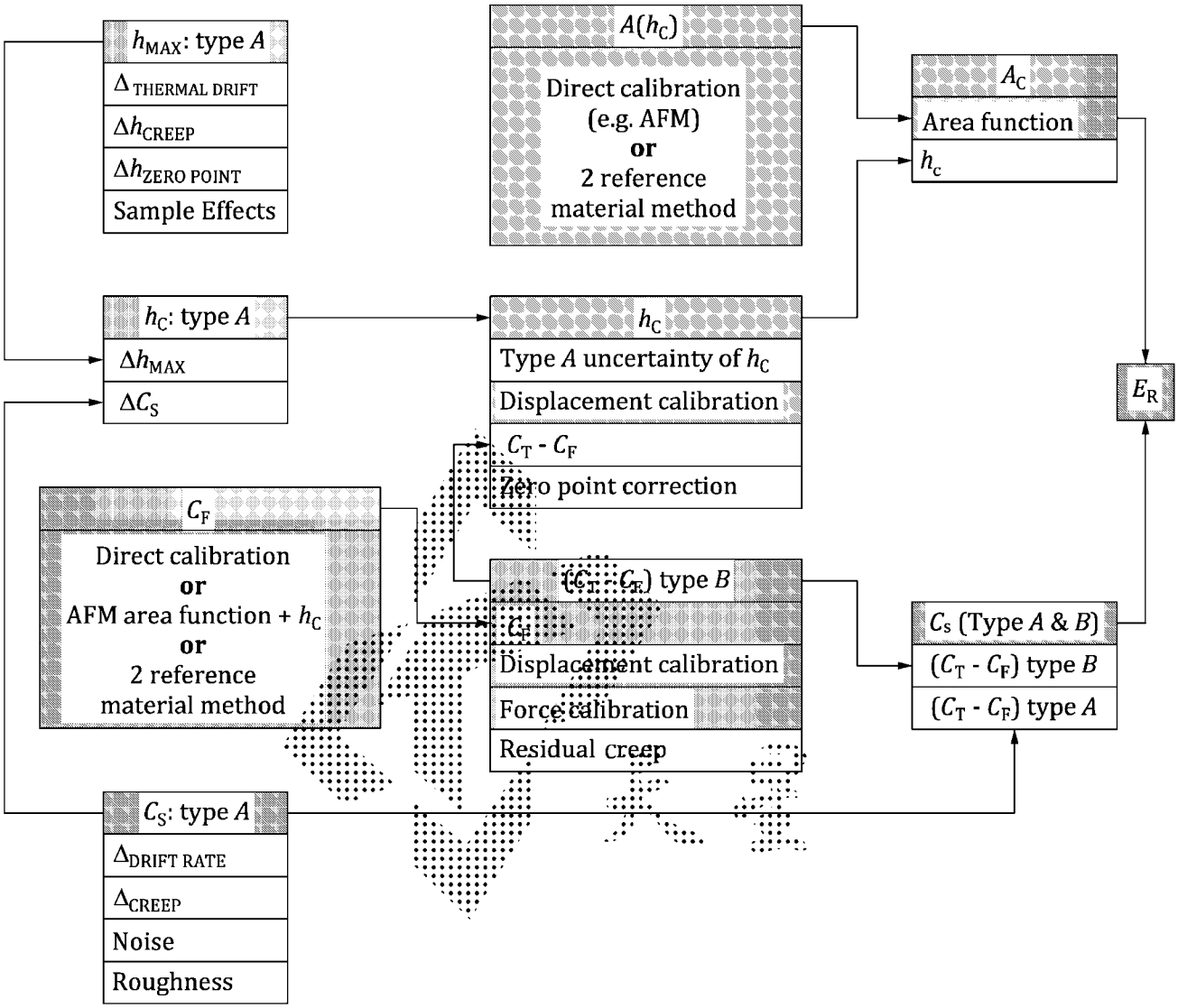

Figure H.1 — Uncertainties flowchart for indentation modulus

These eight uncertainty contributions are then combined to give the total uncertainty budget as follows.

— Contact area uncertainty derives from uncertainties of both the area function and the measured value of contact depth, h_c, which itself is a combination of displacement calibration, zero point uncertainty, etc. As $C_T - C_F$ does not have a one-to-one correlation with h_c, a sensitivity factor, $f_{sens(CT-CF)}$, as given by Formula (H.7), is used to scale its uncertainty.

$$f_{sens(C_T-C_F)} = \frac{0{,}75 \times F_{max}}{h_c} \tag{H.7}$$

— $(C_T - C_F)$ uncertainty has components from the force removal slope uncertainty, frame compliance, displacement calibration, force calibration, and residual creep rate.

It is useful to use a table to calculate the uncertainty for each box in the flow chart and then build up according to Figure H.1 the total combined uncertainty. Be aware that the sensitivity of E_r to A_p is 0,5 since it is the square root of A_p that appears in the formula.

In Table H.2, contact-depth random uncertainty is considered.

Table H.2 — Example table for calculation and combination of uncertainties

h_C random	Sensitivity	Value %	Distribution	Divisor	u
h_{max} random type	1	1	normal	1	1,0
C random type	$0,75 \times F_{max}/h_C$	0,3	normal	1	0,3
combine in quadrature	—	—	normal	1	1,04

H.2.3.3 Hardness analysis

The relationship governing the calculation of hardness is given by Formula (H.8):

$$H_{IT} = \frac{F_{max}}{A(h_c)} \tag{H.8}$$

NOTE The formula gives H_{IT} in MPa. To get H_{IT} in GPa a factor of 10^{-3} is required.

Thus, the calculation of uncertainty of contact area is the same as for the modulus, except that for hardness, the sensitivity is unity as hardness is inversely proportional to contact area. The only additional uncertainty required is the total (random plus systematic) uncertainty in the force. The systematic uncertainty in force is taken from the force calibration certificate. The random uncertainty can be found from the displacement data in the hold periods. The data used to calculate the thermal drift rate is (after correction) normally distributed about a mean value; the random fluctuations being due to vibration, etc. In a feedback-controlled approach, the stiffness of the contact is known and so the random force uncertainty is the stiffness multiplied by the standard deviation of the displacement values. If this method is not possible, then it is possible to use a hold at 90 % force removal, if it is possible to use the final force removal to estimate the contact stiffness. Ultimately, the stiffness of the contact at F_{max} is known and the product of this and the standard deviation of the high-frequency displacement variations in the hold at maximum force (i.e. after removing any underlying creep function) is an estimate of the force noise. Be aware, however, that the sensitivity of this method is much reduced if high stiffness contacts are used.

The combined uncertainty can then be calculated by the flowchart in Figure H.2.

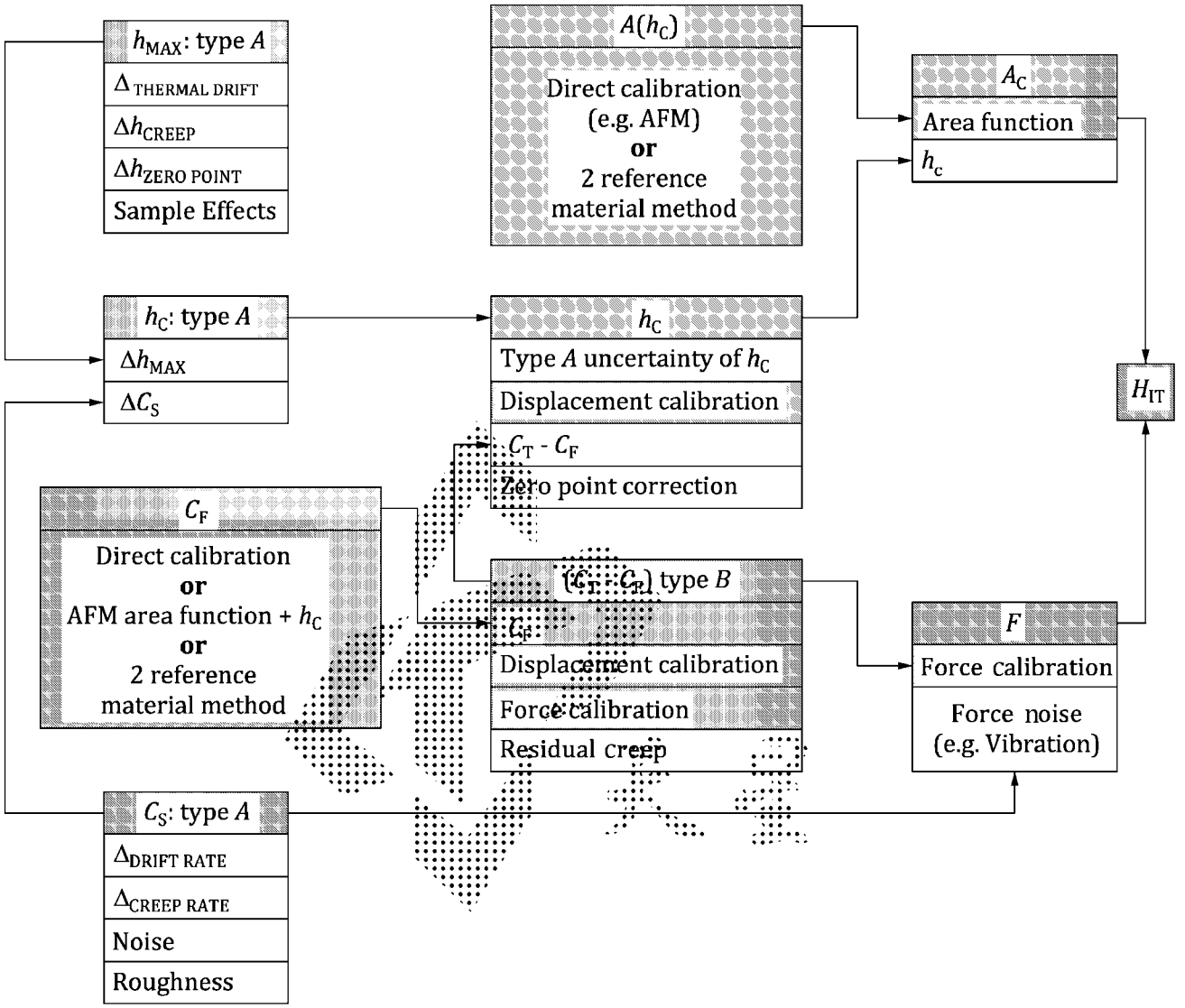

Figure H.2 — Uncertainties flowchart for hardness

Annex I
(normative)

Calculation of radial displacement correction

It is important to understand the effect of this correction on the different calculations performed in indentation analysis. Let an indentation into a material of modulus E produce a contact under force with stiffness S (reciprocal of compliance), and radius a at a contact depth h_c. Let the area function used in analysis be taken to be the real (unloaded) shape of the indenter at the value of h_c (measured from the tip at the centre of the indent).

Let the value of the contact radius obtained from the unloaded area function be a_0. Due to radial dilation, the actual contact radius, a, is smaller than the indenter area function value, a_0, by a factor ($1\text{-}K \times H_{IT,0}/E_{IT,0}$). Thus, correcting for radial dilation yields a corrected contact area value (at a contact depth h_c) of πa^2 that is less than the πa_0^2 value that would be inferred from the shape of the unloaded indenter measured at the same depth by direct methods (e.g. AFM).

Thus, correcting indentation results for radial dilation increases the E and H values as given in Formulae (I.1) and (I.2).

$$H_{IT,1} = H_{IT,0}\left(1 + K \cdot \frac{H_{IT,0}}{E_{IT,0}}\right)^2 \tag{I.1}$$

and

$$E_{r,1} = E_{r,0}\left(1 + K \cdot \frac{H_{IT,0}}{E_{r,0}}\right) \tag{I.2}$$

where $K > 0$ and given by Formula (I.3)

$$K = \frac{(1-2\nu)\cdot(1+\nu)}{2}\cos\theta \tag{I.3}$$

where

$H_{IT,0}$ is the initial estimate of indentation hardness (see A.4.1);

$E_{r,0}$ is the initial estimate of reduced modulus of the indentation contact (see A.5.1);

θ is the angle between the indenter surface and the original surface plane.

The first correction makes the most difference but, since both E and H depend on each other, iteration is required to obtain the best results.

Conversely, when the unloaded indenter area function $A(h_c)$ is derived by indentation of a reference material, the unloaded contact area is calculated using the corrected relationship as given by Formula (I.4).

$$\sqrt{A_{p,F=0}(h_c)} = \frac{\sqrt{\pi}}{2E_r} S \cdot \left(1 + K \cdot \frac{H_{IT}}{E_{r,CRM}}\right)^{-1} \tag{I.4}$$

where

$$H_{IT} = \frac{F}{A_p(h_c)} \tag{I.5}$$

NOTE 1 The formula gives H_{IT} in MPa. To get H_{IT} in GPa a factor of 10^{-3} is required.

NOTE 2 It can be seen that, without this correction, the indentation-derived area function for the same indenter changes as the properties of the reference material used change and, when indenting a material that is not the reference material, causes an error that is a function of the material property difference.

The radial displacement correction is large for elastic materials, such as those typically used for indentation derived area functions.

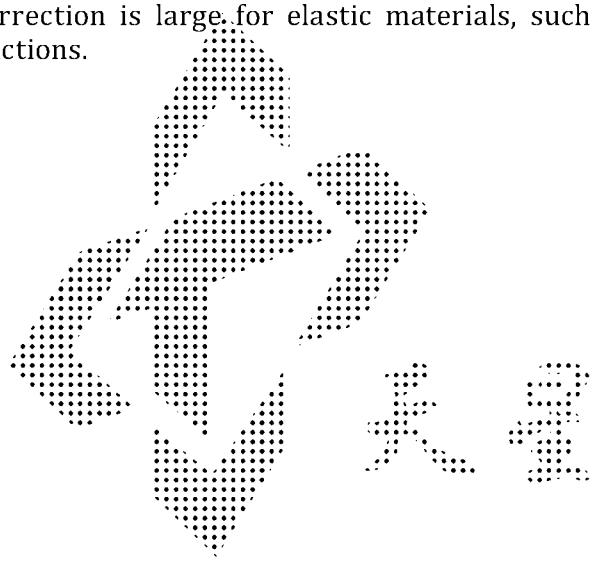

Bibliography

[1] WILDE H.R., & WEHRSTEDT A. Martens hardness HM — An international accepted designation for "Hardness under test force". Zeitschrift Materialprüfung. 2000, **42** pp. 468–470

[2] WEILER W., & BEHNCKE H.-H. Anforderungen an den Eindringkörper für die Universalhärteprüfung. Materialprüfung. 1990, **32** pp. 301–303

[3] MEYER E. Contribution to the Knowledge of Hardness and Hardness Testing. Ver. Dtsch. Ing. 1908, 52 pp. 645–654, 740–748, 835–844

[4] OLIVER W.C., & PHARR G.M. An improved technique for determining hardness and elastic modulus using load and displacement sensing indentation experiments. J. Mater. Res. 1992 June, **7** pp. 1564–1583

[5] SNEDDON I.N. The relation between load and penetration in the axisymmetric Boussinesq problem for a punch of arbitrary profile. Int. J. Eng. Sci. 1965, **3** pp. 47–57

[6] FIELD J.E., & TELLING R.H. The Young modulus and Poisson ratio of diamond. Research Note, PCS Cavendish Laboratory, Dep. of Physics, Madingley Road, Cambridge, CB3 0HE, UK, February 1999

[7] HEERMANT C., & DENGEL D. Zur Abschätzung "klassischer" Werkstoffkennwerte mittels Universalhärteprüfung. Zeitschrift Materialprüfung. 1996, **38** pp. 374–378

[8] BEHNCKE H.-H. Bestimmung der Universalhärte und anderer Kennwerte an dünnen Schichten, insbesondere Hartstoffschichten. Härterei-Technische Mitteilung HTM. 1993, **48** pp. 3–10

[9] GRAU P., ULLNER Ch., BEHNCKE H.-H. Uncertainty of depth sensing hardness. Tagung "Werkstoffprüfung '96" and Zeitschrift Materialprüfung, 39, 9, pp. 362-367, 1997

[10] DOERNER M.F., & NIX W.D. A method for interpreting the data from depth sensing indentation instruments. J. Mater. Res. 1986, **1** pp. 601–609

[11] PETZOLD M., HAGENDORF C., FÜTING M., OLAF J.M. Scanning force microscopy of indenter tips and hardness indentations. VDI Bericht, 1194, 1995

[12] HERRMANN K., JENNETT N.M., WEGENER W., MENEVE J., HASCHE K., SEEMANN R. Progress in determination of the area function of indenters used for nanoindentation. Thin Solid Films. 2000, **377-378** pp. 394–400

[13] CHUDOBA T., & JENNETT N.M. Higher accuracy analysis of instrumented indentation data obtained with pointed indenters. J. Phys. D Appl. Phys. 2008, **41** p. 215407

[14] KING R.B. Elastic analysis of some punch problems for a layered medium. Int. J. Solids Struct. 1987, **23** pp. 1657–1664

[15] CHUDOBA T., & RICHTER F. Investigation of creep behaviour under load during indentation experiments and its influence on hardness and modulus results. Surf. Coat. Tech. 2001, **148** pp. 191–198

[16] SCHWARZER N. The extended Hertzian theory and its use in analysing indentation experiments. Philos. Mag. 2006, **86** pp. 5179–5197

[17] GABAUER W. Manual of Codes of Practice for the Determination of Uncertainties in Mechanical Tests on Metallic Materials, The Estimation of Uncertainties in Hardness Measurements. Project, No. SMT4-CT97-2165, UNCERT COP 14:2000

[18] ISO 4287, *Geometrical Product Specifications (GPS) — Surface texture: Profile method — Terms, definitions and surface texture parameters*

[19] ISO 14577-3:2015, *Metallic materials — Instrumented indentation test for hardness and materials parameters — Part 3: Calibration of reference blocks*

[20] ISO 14577-4, *Metallic materials — Instrumented indentation test for hardness and materials parameters — Part 4: Test method for metallic and non-metallic coatings*

[21] http://www.eurometros.org/metros/packages/

[22] WORIGARD J., DARGENTON J.-C., TROMAS C., AUDURIER V. A New technology for nanohardness measurements: principle and applications. Surf. Coat. Tech. 1998, **100-101** pp. 103–109

ICS 77.040.10
Price based on 46 pages